Integrated sizing and operation of battery energy storage system for prosumers: A comprehensive analysis framework

Yuting Mou[a]

[a]*School of Electrical Engineering, Southeast University, Nanjing 210018, Jiangsu Province, China*

ARTICLE INFO

Keywords:
Energy economics
Capacity expansion
Prosumer
Battery energy storage system
Indivisibility

ABSTRACT

The declining costs of photovoltaic (PV) panels have led to the emergence of residential and commercial prosumers in power systems. PV generation often exhibits uncertainties and temporal mismatches with load profiles, making battery energy storage systems (BESS) a promising solution to enhance the economic value of PV installations. However, existing studies on prosumer BESS mainly focus on uncertainty-aware algorithms, leaving the theoretical understanding of investment cost recovery and operation principles comparatively underdeveloped. This study proposes a framework to comprehensively analyze the impacts of boundary conditions and prosumers' preferences by assuming a perfect foresight, which also serves as a benchmark for algorithm development. The framework relies on two integrated sizing and operation models, where the investment of the BESS is co-optimized with the operation decisions. More specifically, we consider the prosumer under a retail tariff that could comprise both a volumetric energy component and a capacity component, and develop a continuous model to analyze system marginal cost formation, investment cost recovery principles, and internal rate of return (IRR) constraint impacts via Karush-Kuhn-Tucker (KKT) conditions. We then propose a discrete model to evaluate efficiency losses caused by limited BESS configurations in practice. Numerical simulations on an electric vehicle charging station demonstrate that network capacity charges account for 20.4%-62% of total cost savings depending on tariff structure; the optimal energy-to-power ratio ranges from 2.1 hours in the base case to 3.6 hours under high PV generation, and is 2.4 hours in the case with a higher network capacity tariff; IRR constraints reduce optimal investment and require investment horizons of at least 10 years to approach an 8% target; and indivisibility losses are negligible (below 2%) for prosumers with peak demand exceeding 900 kW. This study advances both the theoretical and practical understanding of BESS sizing and operation for prosumers under retail tariffs.

1. Introduction

1.1. Background

Prosumers are playing an increasingly important role in modern power systems, especially as the cost of photovoltaic (PV) panels and battery energy storage systems (BESS) continues to decline steadily. The EU Clean Energy Package empowers active consumers and prosumers as legal participants in the EU energy transition, allowing for the generation, storage, and sale of excess electricity, promoting self-consumption [1]. According to International Renewable Energy Agency, PV costs dropped 90% since 2010 to 0.043 \$/kWh, while battery storage costs plunged 93% to 192 \$/kWh by 2024 [2]. These prosumers, which include households and small-to-medium commercial consumers, typically purchase electricity under retail tariffs set by utilities or aggregators. In liberalized electricity markets, such tariffs usually consist of a competitive energy charge and a regulated network charge. The most common structures are volumetric tariffs, based on total energy consumption (kWh), which may be supplemented by capacity charges calculated from a consumer's peak demand (kW) over a 15-minute to one-hour interval within a billing period. In practice, some utilities, such as Salt River Project in Arizona, and distribution system operators, such as Fluvius in Belgium, have already mandated capacity charges for prosumers with rooftop PV systems as part of their network tariffs [3, 4]. Meanwhile, with BESS costs also falling rapidly, economic potential is emerging for prosumers to store surplus PV generation, avoid low-value exports, and reduce peak demand. These developments raise the question of how to optimally size and operate BESS to maximize economic benefits.

Research on conventional generator sizing and operation is well-established in the capacity expansion framework based on integrated investment-operation models [5, 6], which we also briefly discuss in Appendix A of this paper,

* Corresponding author: Yuting Mou, yutingmou@seu.edu.cn.
ORCID(s): 0000-0002-4536-8015 (Y. Mou)

Table 1
Comparison of representative studies on BESS sizing and / or operation. App: Application scenario; Grid-i: Grid-integrated; Inv: Investment decisions; Op: Operation decisions; Deg: Degradation; Theo: Theoretical analysis for economic insights; WHSLE: Wholesale markets; Opt: Optimization; DN: Distribution network; MG: Microgrid; VT: Volumetric tariff based on kWh; CT: Capacity tariff based on peak kW; RC: Residential and commercial prosumers.

Ref	App	Method	Inv	Op	Deg	Retail	Theo	IRR	Indivisibility	Simulation
[8, 9]	Grid-i	Opt	✔	✔	–	–	–	–	–	IEEE DN
[10]	Grid-i	Opt	✔	✔	–	–	–	✔	✔	Artificial MG
[11]	Grid-i	Fuzzy logic	–	✔	–	VT	–	–	–	Artificial MG
[12]	Grid-i	Opt+DRL	–	✔	–	–	–	–	–	IEEE DN
[13]	Grid-i	Opt	–	✔	–	–	–	–	–	IEEE DN
[14]	Grid-i	Opt	–	✔	–	–	–	–	–	Real area
[15]	Grid-i	Consensus	–	✔	–	–	–	–	–	IEEE MG
[16]	WHSLE	Opt	–	✔	✔	–	–	–	–	UK
[17]	WHSLE	Opt	–	✔	–	–	–	–	–	Europe
[18]	WHSLE	Opt	✔	✔	–	–	–	–	–	IEEE test
[19]	WHSLE	Opt+RL	✔	✔	✔	–	–	–	–	Ireland
[20]	WHSLE	Opt	–	✔	–	–	–	–	–	Artificial
[21]	WHSLE	Opt	–	✔	✔	–	–	–	–	UK
[22]	WHSLE	RL	–	✔	–	–	–	–	–	Germany
[23]	WHSLE	Regime switch	–	✔	✔	–	✔	–	–	NordPool
[24]	WHSLE	Opt	–	✔	–	–	–	–	–	Germany
[25]	WHSLE	Opt	–	✔	–	–	–	–	–	Alberta
[26]	WHSLE	Opt	–	✔	–	–	✔	–	–	France
[27]	WHSLE	Opt	–	✔	–	–	–	–	–	UK
[28, 29]	WHSLE	Opt	✔	✔	–	–	✔	–	–	Artificial
[30]	Prosumer	Opt	✔	–	–	–	–	–	✔	Residential
[31]	Prosumer	Opt	✔	✔	✔	VT+CT	–	✔	–	Public buildings
[32]	Prosumer	Opt	✔	✔	✔	VT	–	✔	–	Residential
[33]	Prosumer	Opt	–	✔	✔	CT	–	✔	–	RC
This	Prosumer	Opt	✔	✔	✔	VT+CT	✔	✔	✔	EV station

but BESS exhibits fundamentally different techno-economic characteristics, making BESS sizing and operation more complex than conventional generation assets and posing challenges to understanding its behavior.

1.2. Literature review

Existing studies on BESS sizing and operation are extensive across the engineering, economics, and operations research literature [7], which can be broadly classified into three main streams according to the application scenarios of BESS.

The first category examines grid-integrated BESS (transmission, distribution, or microgrid level), focusing on operator perspectives for profit maximization or cost minimization, subject to possible network constraints [34]. Representative studies include distribution system BESS siting and sizing with PV productions [8, 9], and sizing problem in the microgrid with specific financial requirement [10]. To tackle uncertainties faced by the BESS during operation, fuzzy logic-based controllers [11], hierarchical operation strategy incorporating deep reinforcement learning [12] and multi-stage stochastic programming model [13] are proposed. Reference [14] further extends the work in [13] by proposing a multi-stage robust model dealing with virtual energy storage. Other studies address specific challenges like network losses through consensus-based algorithms [15]. Our study is conducted from the prosumer's perspective and the BESS is co-located with the prosumer's PV installation, so joint location-sizing as a network-level problem is beyond the current scope.

The second research stream investigates utility-scale BESS directly participating in wholesale markets and aiming to maximize the net profit from the perspective of an investor. Techno-economic assessment for the investment is conducted in [16] and [17] based on different business models, while [18] proposes a distributionally robust chance-constrained program to optimize the investment of BESS through arbitrage in the day-ahead and real-time markets.

Reference [19] restricts the analysis to the the Irish day-ahead market, but the study optimizes both the investment time and BESS capacity size considering future BESS capital expenditure realizations. Additional research explores bidding strategies across various market structures, including the day-ahead market [20, 21], the continuous intraday market [22], the balancing market [23], integrated day-ahead and intraday markets [24], and combined day-ahead and balancing markets [25, 26]. Reference [27] optimizes the operation in a more comprehensive setting, which involves the UK day-ahead and intraday markets, as well as dynamic frequency response services and imbalance settlement. Reference [28] studies the optimal generation mix in power systems with only variable renewable energy and electric energy storage, and evaluates the long-term equilibrium and electricity price structure in the energy market. This analysis is extended to account for the capacity market for long-term storage in [29].

The third and most relevant category concerns small-scale BESS, which typically operate under retail tariffs offered by energy providers [35]. For instance, Reference [30] develops an online energy management tool to determine the optimal size of residential hybrid PV–BESS systems based on prosumers' self-sufficiency expectations. Reference [31] evaluates the economic viability of BESS for public buildings with distributed PV generation in Brazil under a time-of-use (ToU) tariff with contracted power limit, and subsequently extend their analysis to compared residential PV–BESS systems under different tariff schemes, including flat and ToU tariffs [32]. Furthermore, reference [33] conduct a techno-economic analysis of BESS lifetime degradation costs in the optimal scheduling of residential and commercial prosumers, thereby providing a more accurate assessment of profitability.

Despite the extensive literature on various application scenarios as summarized in Table 1, most existing studies mainly conduct numerical simulations and notable efforts are devoted to developing algorithms to deal with various sources of uncertainty.However, theoretical analyses of investment cost recovery and the underlying rationale of operation decisions remain comparatively underdeveloped. In addition, several practical factors are less-discussed for prosumer BESS sizing and operation, including the energy-to-power ratio, battery degradation, the internal rate of return (IRR), and the indivisibility of power conversion system (PCS) and battery modules. Against this background, rather than designing sophisticated uncertainty-aware algorithms, this study proposes a framework for comprehensively analyzing the impacts of boundary conditions and prosumers' preferences, under the assumption of perfect foresight. This assumption offers three distinct advantages over uncertainty-aware alternatives for the purpose of this study. First, it enables tractable KKT analysis, from which closed-form economic principles can be derived analytically, and these insights are generally obscured in stochastic or robust formulations due to scenario-dependent dual variables. Second, the perfect-foresight solution constitutes a theoretical upper bound on achievable BESS savings, providing a benchmark against practical uncertainty-aware algorithms, which a typical approach to evaluate expected value of perfect information [36]. Third, the computational tractability of the perfect-foresight model allows years of hourly data to be optimized exactly, enabling extensive sensitivity analyses across tariff structures, PV capacities, IRR requirements, and prosumer scales that would be computationally challenging under stochastic programming.

The following research gaps remain. First, most prosumer BESS studies rely on numerical simulations without theoretical analysis of investment cost recovery or operation principles, leaving the economic rationale of sizing decisions underexplored. Second, the role of the IRR constraint in shaping optimal BESS sizing has received little attention, despite its practical importance for prosumers seeking project financing. Third, the efficiency losses arising from the indivisibility of commercial BESS configurations have rarely been quantified, making it difficult for practitioners to assess the reliability of continuous approximations. Fourth, the interaction between BESS sizing principles and retail tariff structure, specifically the balance between volumetric and capacity charges, lacks detailed economic analysis. This paper directly addresses these gaps through a unified analytical framework combining theoretical analysis with numerical simulation.

1.3. Contributions and paper organization

The objective of this paper is to develop a comprehensive analysis framework for BESS sizing and operation for prosumers under retail tariffs, providing both theoretical economic insights and practical sizing guidance. Towards this objective, the main contributions are summarized as follows.

- We propose a continuous optimization model that explicitly distinguishes PCS and battery investments as separate continuous decision variables, incorporates calendar and cycling degradation, prosumers' IRR preferences, and both volumetric and capacity retail tariff components. Based on KKT optimality conditions, we derive closed-form expressions for system marginal cost under each operating regime (Proposition 3) and prove that scarcity rents exactly recover the investment costs of the PCS, the battery pack, and the procured network capacity (Proposition 4). To our knowledge, this is the first theoretical framework to establish these cost recovery principles for prosumer BESS under a combined capacity-volumetric tariff. We further characterize how the IRR constraint impacts optimal investment relative to the unconstrained case (Proposition 5).

- We propose a discrete model that captures the limited availability of commercial BESS configurations in practice, with binary investment variables over a set of available PCS and battery module combinations. We derive an upper bound on the resulting indivisibility loss (Proposition 1) and prove that this bound is independent of the number of available BESS models under certain conditions, which is a structural result that has not previously appeared in the prosumer BESS literature.
- Numerical simulations on a real-world EV charging station case study validate theoretical propositions and provide quantitative insights: (i) under high network capacity tariffs, capacity cost savings account for up to 60% of total BESS savings, and the optimal energy-to-power ratio decreases relative to pure-arbitrage scenarios; (ii) IRR constraints reduce optimal BESS investment and require longer investment horizons, as a 10-year horizon is needed to approach an 8% IRR target in the case studied; (iii) indivisibility losses are economically negligible (below 2% of total savings) for prosumers with peak demand above 900 kW, but can reach 13.5% for small prosumers.

Compared to the conventional generator framework reviewed in Appendix A, BESS presents fundamental differences that motivate our theoretical analysis. First, the two-dimensional investment structure (PCS and battery) requires separate cost recovery conditions for each component (Proposition 4 ii-iii). Second, BESS operation is governed by opportunity costs and degradation rather than a fixed marginal cost, leading to different system marginal cost formation (Proposition 3) that cannot be derived from the standard merit-order logic. Third, battery capacity degrades over time, introducing a time-varying effective capacity and a calendar-loss opportunity cost term (Proposition 4 iii) with no analogue in conventional generation. The IRR constraint (Proposition 5) and indivisibility losses (Proposition 1) further distinguish the prosumer BESS problem from the classical capacity expansion setting.

To better convey our theoretical analysis and corroborate the findings with numerical simulations, we adopt a slightly unconventional structure. In Section 2.1, we introduce the mathematical formulation of the continuous model along with its KKT conditions. The theoretical results derived from this model are presented in the form of propositions in Section 3, together with numerical simulations on an EV charging station. Proofs of the propositions are provided in Appendix B. Following the continuous model, Section 2.2 presents the discrete model and analyzes the indivisibility losses. The theoretical and numerical results are discussed in Section 4, where we also offer practical guidance for BESS sizing. Finally, Section 5 concludes the paper and provides directions for future research. The notations are introduced alongside the models and are also summarized in Appendix C.

2. Methods

This study examines a prosumer equipped with PV panels and operating under a retail contract with an energy provider. Drawing on the business model framework established in [35] and currently implemented by some European energy companies [37], along with the tariff design principles from [38], we adopt the following tariff structure: firstly, the prosumer imports electricity at an hourly varying rate, consisting of the day-ahead market clearing price plus a volumetric network tariff, while exports are compensated at a discounted day-ahead price (such as 95% of market price to maintain provider profit margins), also subject to the volumetric network tariff; secondly, the prosumer incurs capacity-based network charges determined by monthly peak import / export levels. We consider an integrated investment-operation framework, which is standard in the capacity expansion literature [5, 39], and we separate the sizing of the PCS and the battery pack to reflect storage duration. The subsequent sections present integrated sizing and operation models that integrate hourly BESS operational constraints with long-term investment decisions. The notations are introduced alongside the models and are also summarized in Appendix C. The workflow of the proposed framework is illustrated in Figure 1.

2.1. The continuous model

The continuous model is formulated as (1)–(6), where the investment decisions for the PCS and battery pack are treated as continuous variables. We present the objective, constraints and the KKT conditions in sequence.

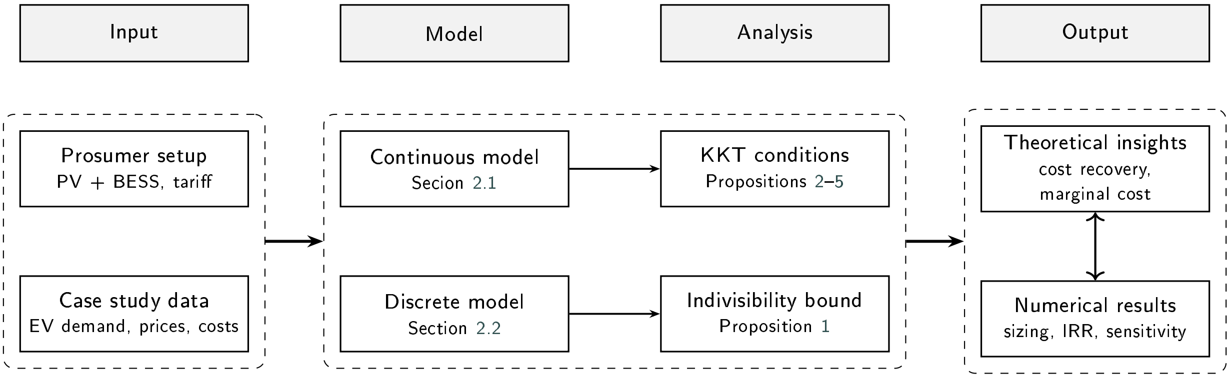

Figure 1: Workflow of the proposed framework. Inputs (prosumer setup and case data) feed the modeling and analysis stage, which includes the continuous and discrete models. The resulting theoretical insights and numerical results mutually corroborate.

2.1.1. Objective

$$\min C^{\text{pcs}} \cdot x^{\text{pcs}} + C^{\text{bat}} \cdot x^{\text{bat}} + \sum_{y\in\mathcal{Y}} \Big(\sum_{m\in\mathcal{M}_y} p_m^{\text{pk}} \cdot \pi_m^{\text{pk}} + \sum_{t\in\mathcal{T}_y} (p_t^{\text{im}} \cdot \pi_t^{\text{im}} - p_t^{\text{ex}} \cdot \pi_t^{\text{ex}}) \Big) \cdot \gamma_y \tag{1}$$

Equation (1) defines the objective function, which aims to minimize the total cost expressed in present value terms. The parameters C^{pcs} and C^{bat} represent the unit costs of the PCS and battery pack, respectively. Therefore, the first two terms correspond to the total investment cost of the BESS with x^{pcs} and x^{bat} denoting the decisions variables of investment capacity. The third term incorporates the monthly network capacity tariff, as well as the hourly power import and export prices, denoted by π_m^{pk}, π_t^{im}, and π_t^{ex}, respectively. This term captures the monthly cost of network capacity procurement, the cost of purchasing electricity from the grid, and the revenue from selling electricity back to the grid. The parameter $\gamma_y = (1+r)^{-y}$ converts the monetary value in year y to its present value via a discount rate r.

2.1.2. Constraints

In this section, we describe several sets of constraints imposed on the continuous model, including internal rate of return, power limits, battery degradation and energy dynamics, and power balance.

2.1.2.1. Internal rate of return

$$(C^{\text{pcs}} \cdot x^{\text{pcs}} + C^{\text{bat}} \cdot x^{\text{bat}}) - \sum_{y\in\mathcal{Y}} \Big(C_y - \sum_{m\in\mathcal{M}_y} p_m^{\text{pk}} \cdot \pi_m^{\text{pk}} - \sum_{t\in\mathcal{T}_y} (p_t^{\text{im}} \cdot \pi_t^{\text{im}} - p_t^{\text{ex}} \cdot \pi_t^{\text{ex}})\Big) \cdot \gamma_y^{\text{irr}} \le 0 \qquad (\lambda) \tag{2}$$

Although the objective is to minimize total costs, a minimum IRR, denoted by r^{irr}, is typically required. This metric is widely used in financial analysis to assess the profitability of investment projects. It is enforced through constraint (2), where parameter C_y denotes the total cost incurred if the BESS is not installed, and the parameter $\gamma_y^{\text{irr}} = (1+r^{\text{irr}})^{-y}$ is calculated based on the target IRR. This constraint requires the net present value of cost savings, discounted at the target IRR, covers the investment cost. This is a standard project-level IRR definition while an annual IRR constraint would be more restrictive and likely render the problem infeasible in many cases. Generally, r reflects inflation or currency depreciation, whereas r^{irr} is set higher than the interest rate on loans to ensure a positive net return. Consequently, $\gamma_y^{\text{irr}} < \gamma_y$.

2.1.2.2. Power limits

$$p_t^{\text{ch}} - x^{\text{pcs}} \le 0, t \in \mathcal{T} \qquad (\lambda_t^{\text{ch}}) \tag{3a}$$

$$p_t^{\text{dis}} - x^{\text{pcs}} \le 0, t \in \mathcal{T} \qquad (\lambda_t^{\text{dis}}) \tag{3b}$$

$$p_t^{\text{im}} - p_m^{\text{pk}} \le 0, t \in \mathcal{T}_m, m \in \mathcal{M} \qquad (\lambda_t^{\text{im}}) \tag{3c}$$

$$p_t^{\text{ex}} - p_m^{\text{pk}} \leq 0, t \in \mathcal{T}_m, m \in \mathcal{M} \qquad (\lambda_t^{\text{ex}}) \tag{3d}$$

Constraints (3a)–(3b) limit the charge power p_t^{ch} and discharge power p_t^{dis} to the installed PCS capacity x^{pcs}, which is also decided by the model. Similarly, constraints (3c)–(3d) restrict the import and export powers, p_t^{im} and p_t^{ex}, to the monthly peak demand p_m^{pk}, based on which the prosumer pays network capacity charges.

2.1.2.3. Battery degradation and energy dynamics

$$x^{\text{bat}} - x^{\text{bat}} \cdot \Delta h_t^{\text{cal}} - \alpha \cdot (p_t^{\text{ch}} + p_t^{\text{dis}}) - x_t^{\text{bat}} = 0, t = 1 \qquad (\nu_1^x) \tag{4a}$$

$$x_{t-1}^{\text{bat}} - x^{\text{bat}} \cdot \Delta h_t^{\text{cal}} - \alpha \cdot (p_t^{\text{ch}} + p_t^{\text{dis}}) - x_t^{\text{bat}} = 0, t \in \mathcal{T}, t > 1 \qquad (\nu_t^x) \tag{4b}$$

$$h^{\dagger} \cdot x^{\text{bat}} - x_t^{\text{bat}} \leq 0, t \in \mathcal{T} \qquad (\lambda_t^x) \tag{4c}$$

The battery energy capacity x^{bat} degrades over time due to both calendar and cycling losses, as modeled by (4a) and (4b). The remaining energy capacity at time t is denoted by x_t^{bat}, and its degradation is tracked using the state of health (SOH), expressed as a percentage. Calendar loss at time t is denoted by Δh_t^{cal}, while cycling loss at t is assumed to be linearly proportional to the energy throughput, as a function of charge and discharge power. This linear approximation is also supported by large multi-year field measurement data [40], and it enables the KKT analysis. Both Δh_t^{cal} and the degradation coefficient α are parameters calibrated from experimental data. When the state of health (SOH) falls below a specified threshold, the BESS is considered to have reached end-of-life. Thus, constraint (4c) ensures that the SOH remains above the threshold $h^{\dagger}$ over the investment horizon. Note that we assume PCS does not degrade in our model, which is justified by PCS having negligible degradation over typical investment horizons relative to battery packs.

$$x^{\text{bat}} \cdot s_0 + p_t^{\text{ch}} \cdot \eta^{\text{ch}} - p_t^{\text{dis}} / \eta^{\text{dis}} - e_t = 0, t = 1 \qquad (\nu_1^e) \tag{5a}$$

$$e_{t-1} + p_t^{\text{ch}} \cdot \eta^{\text{ch}} - p_t^{\text{dis}} / \eta^{\text{dis}} - e_t = 0, t \in \mathcal{T}, t > 1 \qquad (\nu_t^e) \tag{5b}$$

$$e_t - x_t^{\text{bat}} \cdot \overline{s} \leq 0, t \in \mathcal{T} \qquad (\overline{\lambda}_t^e) \tag{5c}$$

$$x_t^{\text{bat}} \cdot \underline{s} - e_t \leq 0, t \in \mathcal{T} \qquad (\underline{\lambda}_t^e) \tag{5d}$$

Equations (5a) and (5b) model the energy dynamics of the BESS. The energy level e_t increases due to charging and decreases due to discharging, accounting for charging and discharging efficiencies η^{ch} and η^{dis}, respectively. The state of charge (SOC), with the initial value denoted by s_0, remains within specified bounds $\underline{s}$ and $\overline{s}$, as enforced by constraints (5c) and (5d).

2.1.2.4. Power balance

$$p_t^{\text{ch}} - p_t^{\text{dis}} + D_t^{\text{net}} - p_t^{\text{im}} + p_t^{\text{ex}} = 0, t \in \mathcal{T} \qquad (\nu_t^{\text{sys}}) \tag{6a}$$

$$x^{\text{pcs}}, x^{\text{bat}}, p_m^{\text{pk}}, p_t^{\text{dis}}, p_t^{\text{ch}}, p_t^{\text{ex}}, p_t^{\text{im}}, x_t^{\text{bat}} \geq 0 \tag{6b}$$

The hourly power balance is ensured by (6a), where the supply consists of power imported from the grid and power discharged from the BESS. The demand includes prosumer net demand accounting for PV generation, BESS charging demand, and power exported to the grid. Finally, (6b) imposes non-negativity constraints on all decision variables.

2.1.3. KKT conditions

The KKT conditions for the continuous model are provided in (7a)-(7s). These equations offer deeper insight into the behavior of the prosumer, and several propositions are developed accordingly in Section 3. In Propositions 2-4, we consider a simplified setting in which the IRR constraint (2) is disregarded, implying $\lambda = 0$. Additionally, the discount rate is assumed to be zero for notational simplicity, leading to $\gamma_y = 1$. The derivation process of Propositions 2-4 still holds for non-zero discount rate.

$$0 \leq x^{\text{pcs}} \perp C^{\text{pcs}} + \lambda \cdot C^{\text{pcs}} - \sum_{t \in \mathcal{T}} \lambda_t^{\text{ch}} - \sum_{t \in \mathcal{T}} \lambda_t^{\text{dis}} \geq 0 \tag{7a}$$

$$0 \le x^{\text{bat}} \perp C^{\text{bat}} + \lambda \cdot C^{\text{bat}} + \sum_{t\in\mathcal{T}} \lambda_t^x \cdot h^\dagger - \sum_{t\in\mathcal{T}} v_t^x \cdot \Delta h_t^{\text{cal}} + v_1^x + s_0 \cdot v_1^e \ge 0 \tag{7b}$$

$$0 \le p_m^{\text{pk}} \perp \pi^{\text{pk}} \cdot \gamma_y + \lambda \cdot \pi^{\text{pk}} \cdot \gamma_y^{\text{irr}} - \sum_{t\in\mathcal{T}_m} \lambda_t^{\text{im}} - \sum_{t\in\mathcal{T}_m} \lambda_t^{\text{ex}} \ge 0, m \in \mathcal{M}_y, y \in \mathcal{Y} \tag{7c}$$

$$0 \le p_t^{\text{im}} \perp \pi_t^{\text{im}} \cdot \gamma_y + \lambda \cdot \pi_t^{\text{im}} \cdot \gamma_y^{\text{irr}} + \lambda_t^{\text{im}} - v_t^{\text{sys}} \ge 0, t \in \mathcal{T}_y, y \in \mathcal{Y} \tag{7d}$$

$$0 \le p_t^{\text{ex}} \perp -\pi_t^{\text{ex}} \cdot \gamma_y - \lambda \cdot \pi_t^{\text{ex}} \cdot \gamma_y^{\text{irr}} + \lambda_t^{\text{ex}} + v_t^{\text{sys}} \ge 0, t \in \mathcal{T}_y, y \in \mathcal{Y} \tag{7e}$$

$$0 \le p_t^{\text{ch}} \perp \lambda_t^{\text{ch}} - \alpha \cdot v_t^x + \eta^{\text{ch}} \cdot v_t^e + v_t^{\text{sys}} \ge 0, t \in \mathcal{T} \tag{7f}$$

$$0 \le p_t^{\text{dis}} \perp \lambda_t^{\text{dis}} - \alpha \cdot v_t^x - v_t^e/\eta^{\text{dis}} - v_t^{\text{sys}} \ge 0, t \in \mathcal{T} \tag{7g}$$

$$0 \le x_t^{\text{bat}} \perp -v_t^x + v_{t+1}^x - \lambda_t^x - \overline{s} \cdot \overline{\lambda}_t^e + \underline{s} \cdot \underline{\lambda}_t^e \ge 0, t \in \mathcal{T}, t < T \tag{7h}$$

$$0 \le x_t^{\text{bat}} \perp -v_t^x - \lambda_t^x - \overline{s} \cdot \overline{\lambda}_T^e + \underline{s} \cdot \underline{\lambda}_t^e \ge 0, t = T \tag{7i}$$

$$0 < e_t \perp -v_t^e + v_{t+1}^e + \overline{\lambda}_t^e - \underline{\lambda}_t^e \ge 0, t \in \mathcal{T}, t < T \tag{7j}$$

$$0 < e_t \perp -v_t^e + \overline{\lambda}_t^e - \underline{\lambda}_t^e \ge 0, t = T \tag{7k}$$

$$0 \le \lambda \perp \sum_{y\in\mathcal{Y}} \big(C_y - \sum_{m\in\mathcal{M}_y} p_m^{\text{pk}} \cdot \pi^{\text{pk}} - \sum_{t\in\mathcal{T}_y} (p_t^{\text{im}} \cdot \pi_t^{\text{im}} - p_t^{\text{ex}} \cdot \pi_t^{\text{ex}})\big) \cdot \gamma_y^{\text{irr}} - (C^{\text{pcs}} \cdot x^{\text{pcs}} + C^{\text{bat}} \cdot x^{\text{bat}}) \ge 0 \tag{7l}$$

$$0 \le \lambda_t^{\text{ch}} \perp x^{\text{pcs}} - p_t^{\text{ch}} \ge 0, t \in \mathcal{T} \tag{7m}$$

$$0 \le \lambda_t^{\text{dis}} \perp x^{\text{pcs}} - p_t^{\text{dis}} \ge 0, t \in \mathcal{T} \tag{7n}$$

$$0 \le \lambda_t^{\text{im}} \perp p_m^{\text{pk}} - p_t^{\text{im}} \ge 0, t \in \mathcal{T}_m, m \in \mathcal{M} \tag{7o}$$

$$0 \le \lambda_t^{\text{ex}} \perp p_m^{\text{pk}} - p_t^{\text{ex}} \ge 0, t \in \mathcal{T}_m, m \in \mathcal{M} \tag{7p}$$

$$0 \le \lambda_t^x \perp x^{\text{bat}} - h^\dagger \cdot x_t^{\text{bat}} \ge 0, t \in \mathcal{T} \tag{7q}$$

$$0 \le \overline{\lambda}_t^e \perp x_t^{\text{bat}} \cdot \overline{s} - e_t \ge 0, t \in \mathcal{T} \tag{7r}$$

$$0 \le \underline{\lambda}_t^e \perp e_t - x_t^{\text{bat}} \cdot \underline{s} \ge 0, t \in \mathcal{T} \tag{7s}$$

2.2. The discrete model and the indivisibility loss

In the previous section, we have assumed both PCS and battery pack investment decisions could take continuous values. However, in practice, the PCS module and battery pack have a limited number of models, and manufacturers assemble these modules into various BESS configurations. In this section, we propose a discrete model and analyze the economic losses due to this indivisibility.

Compared to the continuous model (1)–(6), we introduce a set of possible BESS models $i \in \mathcal{I}$ where each is associated with investment cost C_i^{es}, rated power capacity $p_i^\diamond$ and rated energy capacity $x_i^\diamond$. We also introduce binary variables u_i to indicate whether a particular BESS model is invested in. Note the prosumer is allowed to invest in more than one model. Other decision variables are similar to those in the continuous model, except for the introduction of subscript i. Constraints (8f)-(8o) are imposed for each i, but (8b) and (8c) are distinct from (2) and (6a) because the investment refers to all invested BESS models. When multiple BESS models are invested, their combined charge / discharge power is aggregated in the power balance constraint (8c), and each unit independently satisfies its own operating constraints (8f)-(8n). The coordination between units is implicit in the shared power balance (8c) and the shared network capacity constraints (8d)-(8e).

$$\min \sum_{i\in\mathcal{I}} C_i^{\text{es}} \cdot u_i + \sum_{y\in\mathcal{Y}} \Big(\sum_{m\in\mathcal{M}_y} p_m^{\text{pk}} \cdot \pi_m^{\text{pk}} + \sum_{t\in\mathcal{T}_y} (p_t^{\text{im}} \cdot \pi_t^{\text{im}} - p_t^{\text{ex}} \cdot \pi_t^{\text{ex}})\Big) \cdot \gamma_y \tag{8a}$$

$$\text{s.t.} \sum_{i\in\mathcal{I}} C_i^{\text{es}} \cdot u_i - \sum_{y\in\mathcal{Y}} \big(C_y - \sum_{m\in\mathcal{M}_y} p_m^{\text{pk}} \cdot \pi_m^{\text{pk}} - \sum_{t\in\mathcal{T}_y} (p_t^{\text{im}} \cdot \pi_t^{\text{im}} - p_t^{\text{ex}} \cdot \pi_t^{\text{ex}})\big) \cdot \gamma_y^{\text{irr}} \le 0 \tag{8b}$$

$$\sum_{i\in\mathcal{I}} (p_{i,t}^{\text{ch}} - p_{i,t}^{\text{dis}}) + D_t^{\text{net}} = p_t^{\text{im}} - p_t^{\text{ex}}, t \in \mathcal{T} \tag{8c}$$

$$p_t^{\text{im}} - p_m^{\text{pk}} \le 0, t \in \mathcal{T}_m, m \in \mathcal{M} \tag{8d}$$

$$p_t^{\mathrm{ex}} - p_m^{\mathrm{pk}} \leq 0, t \in \mathcal{T}_m, m \in \mathcal{M} \tag{8e}$$
$$p_{i,t}^{\mathrm{ch}} - p_i^{\diamond} \cdot u_i \leq 0, i \in \mathcal{I}, t \in \mathcal{T} \tag{8f}$$
$$p_{i,t}^{\mathrm{dis}} - p_i^{\diamond} \cdot u_i \leq 0, i \in \mathcal{I}, t \in \mathcal{T} \tag{8g}$$
$$h^{\dagger} \cdot x_i^{\diamond} \cdot u_i - x_{i,t} \leq 0, i \in \mathcal{I}, t \in \mathcal{T} \tag{8h}$$
$$x_i^{\diamond} \cdot u_i \cdot (1 - h_t^{\mathrm{cal}}) - \alpha \cdot (p_{i,t}^{\mathrm{ch}} + p_{i,t}^{\mathrm{dis}}) - x_{i,t} = 0, i \in \mathcal{I}, t = 1 \tag{8i}$$
$$x_{i,t-1} - x_i^{\diamond} \cdot u_i \cdot \Delta h_t^{\mathrm{cal}} - \alpha \cdot (p_{i,t}^{\mathrm{ch}} + p_{i,t}^{\mathrm{dis}}) - x_{i,t} = 0, i \in \mathcal{I}, t > 1, \tag{8j}$$
$$x_i^{\diamond} \cdot u_i \cdot s_0 + p_{i,t}^{\mathrm{ch}} \cdot \eta^{\mathrm{ch}} - p_{i,t}^{\mathrm{dis}} / \eta^{\mathrm{dis}} - e_{i,t} = 0, i \in \mathcal{I}, t = 1 \tag{8k}$$
$$e_{i,t-1} + p_{i,t}^{\mathrm{ch}} \cdot \eta^{\mathrm{ch}} - p_{i,t}^{\mathrm{dis}} / \eta^{\mathrm{dis}} = e_{i,t}, i \in \mathcal{I}, t > 1 \tag{8l}$$
$$e_{i,t} - x_{i,t} \cdot \overline{s}_i \leq 0, i \in \mathcal{I}, t \in \mathcal{T} \tag{8m}$$
$$x_{i,t} \cdot \underline{s}_i - e_{i,t} \leq 0, i \in \mathcal{I}, t \in \mathcal{T} \tag{8n}$$
$$u_i \in \{0, 1\}, p_{i,t}^{\mathrm{dis}}, p_{i,t}^{\mathrm{ch}}, x_{i,t} \geq 0, i \in \mathcal{I}, t \in \mathcal{T} \tag{8o}$$
$$p_m^{\mathrm{pk}}, p_t^{\mathrm{ex}}, p_t^{\mathrm{im}} \geq 0, m \in \mathcal{M}, t \in \mathcal{T} \tag{8p}$$

The binary variables could incur economic losses, which we define as *Indivisibility Loss* in the following.

Definition 1 (Indivisibility Loss). *The optimal objective value of Problem (8) is denoted as $P^{\star}$ and that of its linear relaxation as $P^{\mathrm{lr},\star}$, the indivisibility loss IL is expressed as*

$$0 \leq IL = P^{\star} - P^{\mathrm{lr},\star}. \tag{9}$$

Since the dual problem of relaxed version of Problem (8) is also a dual[1] of (8), Definition 1 implies the duality gap of problem (8) equals the indivisibility loss. This observation provides a way to bound the indivisibility loss.

Proposition 1. *The bound on the indivisibility loss is independent of the number of BESS models if I is larger than $T + 1$.*

The proof of this proposition is available in Appendix B.1. It should be noted that the practical usefulness of this bound depends on the model's time horizon T. For representative-day models with $T = 24$ or $T = 96$, the bound is tight enough to provide meaningful guarantees without solving the integer program. For the full-year hourly model used in this study ($T = 8760$), the bound becomes too loose to be directly informative, and numerical estimation of IL via comparison of Problem (8) and its linear relaxation is more appropriate.

3. Results

This section presents theoretical results along with a case study of an EV charging station as the prosumer for illustration. The proofs of the propositions are also provided in Appendix B.

3.1. Data and assumptions

The station is equipped with 80 kW rated PV panels and utilizes the hourly demand profile from a real-world station. Figure 2 plots the net demand of one year and each hour corresponds to the net demand in all days at the same hour, which exhibits notable fluctuations ranging from -57.6 to 500.3 kW. The charging station data is available from [42].

The prosumer operates under a retail contract with the following pricing structure. The import price consists of the day-ahead market clearing price plus a 0.05 €/kWh volumetric network tariff. The export price is set at 0.95 times the market price minus the same volumetric network tariff. In addition, the prosumer pays a monthly network capacity charge of 1 €/kW per month based on the monthly peak import or export power. As the network tariffs differ significantly among various countries [3, 43], we use these values as the base case and sensitivity analysis are

[1] The dual of mixed-integer linear problem comes in various forms and the dual of its linear relaxation is one of them [41].

Table 2
Overview of numerical simulations conducted in the study.

Cases	Motivation	$h^{\dagger}$	r	IRR	Section
A-70	The base case for illustrating Propositions 2-4.	70%	0%	0%	3.2
A-70-HighCT	Evaluating impacts of increasing network capacity tariff, reducing network volumetric tariff and removing the network volumetric tariff for exports.	70%	0%	0%	3.2
A-70-NoCT	Evaluating impacts of removing the network capacity tariff.	70%	0%	0%	3.2
A-70-LowDA	Evaluating impacts of lower day-ahead market prices.	70%	0%	0%	3.2
A-70-HighPV	Evaluating impacts of more PV installations.	70%	0%	0%	3.2
A-75	Illustration of Proposition 4 with a less advanced battery.	75%	0%	0%	3.2
A-70-LowIC	Evaluating impacts of lower BESS investment costs.	70%	0%	0%	3.3
B-3-0	Illustration of Proposition 5 without IRR requirement.	70%	3%	0%	3.3
B-3-8	Illustration of Proposition 5 with IRR requirement.	70%	3%	8%	3.3-3.4
C-3-8	Evaluating economic losses due to indivisibility.	70%	3%	8%	3.4

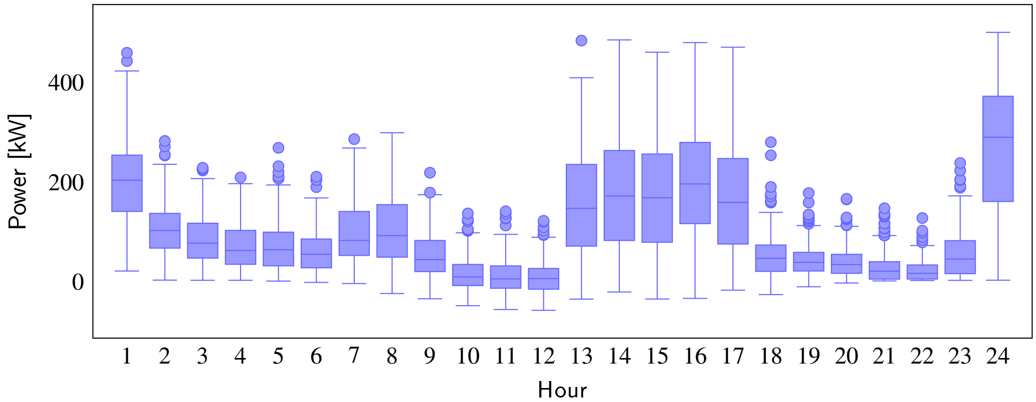

Figure 2: Boxplots of the net demand (aggregated EV charging demand minus PV generation) of each hour over the year.

conducted. Financial parameters include a discount rate of 3% and IRR of 8% where applicable, which reflect common project finance assumptions for low-risk energy investments.

Regarding the BESS parameters, in the continuous model, the PCS and battery pack investment cost is 120 €/kW and 150 €/kWh, respectively. This reflects the typical cost of small- to medium-sized BESS in 2025, and a sensitivity analysis is conducted assuming a 20% cost reduction. In the discrete model, because the configuration of PCS and battery modules differs notably among manufacturers, we assume the set of available sizes for PCS is 5, 10, 20, 40, 80, 160, and 320 kW, and for battery, 5, 10, 20, 40, 80, 160, 320, and 640 kWh. The BESS assembles different PCS and battery pack models, and the cost is the sum of them. The set $\mathcal{I}$ is the Cartesian product of these two sets. In order to focus on indivisibility losses, we maintain identical per-unit costs across both models. Technical specifications include equal charge / discharge efficiency ($\eta^{\text{ch}} = \eta^{\text{dis}} = 0.95$), SOC with an initial value $s_0 = 0.5$ and operating between $\underline{s} = 0.1$ and $\overline{s} = 0.9$, and end-of-life SOH threshold $h^{\dagger} = 70\%$. The calendar loss and cycling loss coefficients are calibrated based on experimental data provided by the manufacturer.

In the following, we first analyze the dual variables based on the continuous model (1)–(6), with a focus on the system marginal cost and scarcity rent, in order to understand BESS sizing and operation. The impact of the IRR constraint would be evaluated across various investment horizons. Finally, the magnitude of the indivisibility loss would be assessed based on the discrete model (8). In Propositions 2-4, we consider a simplified setting in which the IRR constraint (2) is disregarded and the discount rate is assumed to be zero, implying $\lambda = 0$ and $\gamma_y = 1$. The derivation process still holds for a non-zero discount rate. We provide an overview of the numerical simulations in Table 2. It should be noted that the quantitative results derived from the numerical simulations are inherently specific to the EV charging station context. Prosumers with different load profiles, such as residential households or commercial buildings, may yield different optimal sizing decisions and cost breakdowns. However, the qualitative economic principles established through the KKT analysis follow directly from the mathematical structure of the optimization problem and are therefore general, holding for any prosumer type and tariff structure that fits within the modeling framework. Additionally, some sensitivity analyses are conducted to generalize the quantitative results, which are also consolidated by the analytical results.

3.2. Analysis of system marginal cost and scarcity rent

In this section, we conduct various case studies with an investment horizon of 10 years based on the continuous model (1)-(6). The discount rate and IRR constraint are omitted to focus our analysis on the prosumer.

3.2.1. Economic interpretations of dual variables

This section introduces the relationships among several dual variables and their economic interpretations, which will be used in subsequent propositions.

Proposition 2. *Given the KKT conditions in equations (7a)-(7s), the following relationships hold:*

(i) $\lambda_t^x = 0$ *for* $t < T$ *and* $\lambda_t^x \geq 0$ *for* $t = T$.

(ii) $v_t^e = \sum_{\tau=t}^T (\overline{\lambda}_\tau^e - \underline{\lambda}_\tau^e)$.

(iii) $v_t^x = -\lambda_T^x + \sum_{\tau=t}^T (-\overline{s} \cdot \overline{\lambda}_\tau^e + \underline{s} \cdot \underline{\lambda}_\tau^e)$.

Since the BESS is retired once the SOH reaches the threshold $h^\dagger$, the Lagrange multiplier λ_T^x, associated with (4c) at T, reflects the marginal value of having a more durable BESS capable of operating under a lower $h^\dagger$. This multiplier is a useful indicator for prosumers, as greater durability allows the BESS to sustain more cycles, though typically at a higher purchase cost. In case *A-70*, h_T falls to 72% and $\lambda_T^x = 0$, meaning that a BESS with $h^\dagger = 70\%$ is unnecessary because the battery remains operational until the end of the investment horizon. By contrast, in case *A-75*, where $h^\dagger = 75\%$ representing a less advanced battery pack, h_T reaches 75% and $\lambda_T^x = 154.98$, representing the marginal benefit of investing in a more durable BESS. This tipping-point behavior of the SOH constraint, where λ_T^x jumps discontinuously from zero to a positive value when the constraint binds, reflects a structural change in the optimal solution in the sense that the battery lifetime now imposes scarcity, altering both the investment sizing and the battery cost decomposition in Proposition 4 (iii).

Both (ii) and (iii) involve the dual variables $\overline{\lambda}_t^e$ and $\underline{\lambda}_t^e$, which are positive only when the upper or lower bounds of the energy capacity constraints (5c) and (5d) are binding. Therefore, they provide a relatively clearer interpretation indicating energy capacity scarcity. The dual variable v_t^e is associated with the energy dynamics constraint, equals the sum of $\overline{\lambda}_t^e - \underline{\lambda}_t^e$ from t to T, representing the opportunity cost of charging or discharging the BESS. The variable v_t^x, associated with the energy capacity degradation constraint, reflects the cost of energy capacity loss due to degradation.

3.2.2. System marginal cost

Proposition 3. *The system marginal cost* v_t^{sys} *is determined by the operation status. The following conditions hold:*

(i) If the prosumer is importing within the network capacity limit ($0 < p_t^{\text{im}} < p_m^{\text{pk}}$)*, the system marginal cost is equal to the import price, i.e.,* $v_t^{\text{sys}} = \pi_t^{\text{im}}$. *If the capacity limit is reached, a scarcity rent* λ_t^{im} *is generated, such that* $v_t^{\text{sys}} = \pi_t^{\text{im}} + \lambda_t^{\text{im}}$.

(ii) If the prosumer is exporting within the network capacity limit, the system marginal cost is equal to the export price, i.e., $v_t^{\text{sys}} = \pi_t^{\text{ex}}$. *If the capacity limit is reached, a scarcity rent* λ_t^{ex} *is generated, such that* $v_t^{\text{sys}} = \pi_t^{\text{ex}} + \lambda_t^{\text{ex}}$.

(iii) If the BESS is charging within the PCS capacity limit ($0 < p_t^{\text{dis}} < x^{\text{pcs}}$)*, the system marginal cost is given by* $v_t^{\text{sys}} = \alpha \cdot v_t^x - \eta^{\text{ch}} \cdot v_t^e$. *This reflects both the opportunity cost and the degradation cost of the BESS. Further, we can derive* $v_t^{\text{sys}} = -(\alpha \cdot \overline{s} + \eta^{\text{ch}}) \cdot \sum_{\tau=t}^T \overline{\lambda}_\tau^e + (\alpha \cdot \underline{s} + \eta^{\text{ch}}) \cdot \sum_{\tau=t}^T \underline{\lambda}_\tau^e - \alpha \cdot \lambda_T^x$*, which is directly related to the energy capacity scarcity* $\overline{\lambda}_t^e$ *and* $\underline{\lambda}_t^e$. *Otherwise, a scarcity rent* λ_t^{ch} *is generated.*

(iv) If the BESS is discharging within the PCS capacity limit, the system marginal cost is given by $v_t^{\text{sys}} = -\alpha \cdot v_t^x - v_t^e / \eta^{\text{dis}} = (\alpha \cdot \overline{s} - 1/\eta^{\text{dis}}) \cdot \sum_{\tau=t}^T \overline{\lambda}_\tau^e - (\alpha \cdot \underline{s} + 1/\eta^{\text{dis}}) \cdot \sum_{\tau=t}^T \underline{\lambda}_\tau^e + \alpha \cdot \lambda_T^x$. *Otherwise, a scarcity rent* λ_t^{dis} *is generated.*

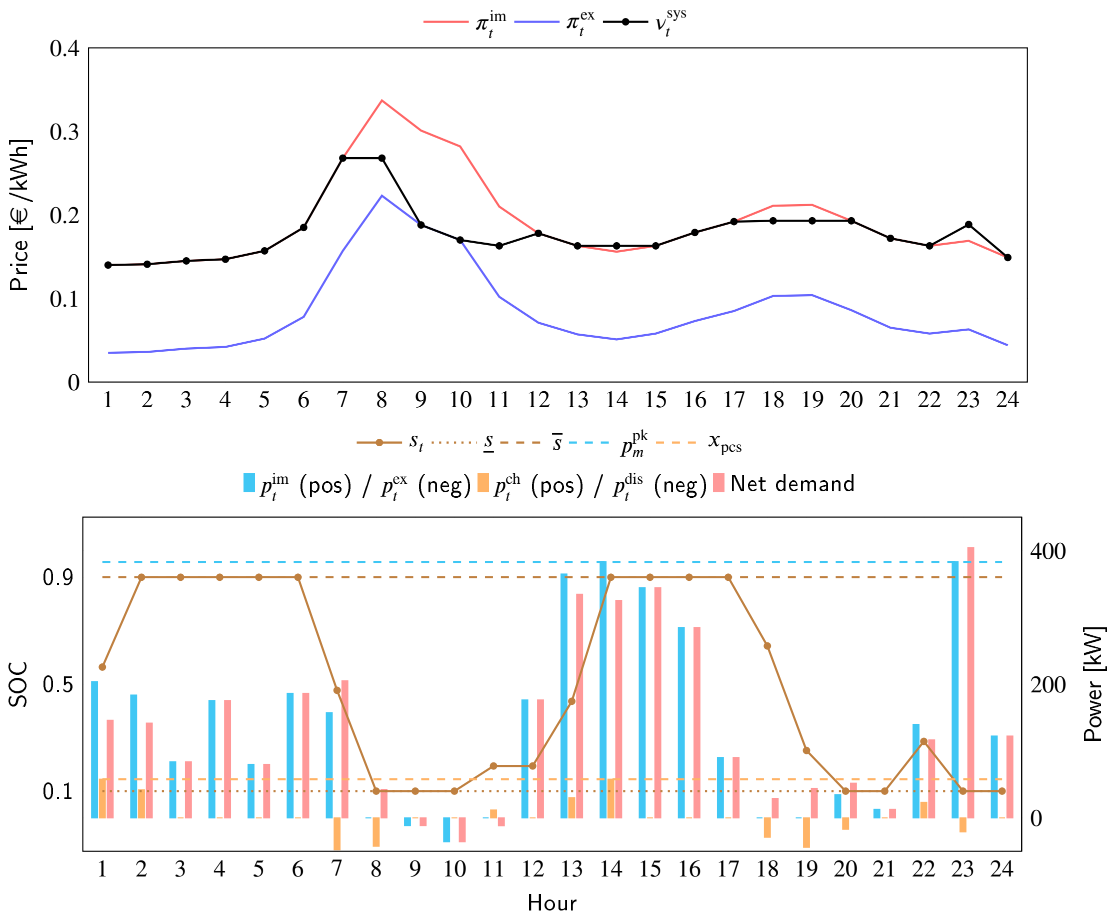

Figure 3: Operation status of the prosumer on a representative day. The upper panel compare the import price, export price and system marginal cost. In the lower panel, the brown solid curve shows the evolution of the SOC within the bounds, indicated by the the brown dashed and dotted curves (left y-axis), while the bars show the import / export (negative) and charge / discharge (negative) decisions, as well as the net demand (right y-axis).

Analysis of the operation shows that the benefits of BESS mainly arise from energy arbitrage and peak demand reduction. In the former case, the BESS can store excess PV generation for later use to meet demand or for export to the grid. Alternatively, it can charge from the grid at low prices and discharge at higher prices, but it requires that the import price be sufficiently lower than the export price to cover the margin, which is challenging due to volumetric network tariffs on exports under our retail tariff assumption. In the latter case, reducing peak demand lowers network capacity charges, which occurs in hours when peak capacity is reached. Figure 3 illustrates BESS operation by comparing system marginal cost with import and export prices on a representative day, consistent with Proposition 3.

- During hours 1-7, 12-13, 15-17, 20-22 and 24, the system price is equal to the import price.
  - In hour 1, the import price is relatively low. The prosumer imports within the network capacity limit and charges at the PCS capacity. Therefore, the import price sets the system marginal cost, corresponding to part (i) of Proposition 3. Meanwhile, a scarcity rent is generated to cover the investment cost of the PCS, which will be discussed later.
  - In hours 2, 13 and 22, the import prices are also relatively low. Both charging and importing are within the capacity limit, so both the BESS and import prices set the system marginal cost, in line with parts (i) and (iii) of Proposition 3.

Table 3
Breakdown of the operation status and cost savings of the BESS across various cases with *given* investments.

Cases	*A-70*	*A-70-HighCT*	*A-70-NoCT*	*A-70-HighPV*
Status [% of all hours]				
Not in operation	60.4	64.3	62.2	59.3
Import peak reduction	1.3	1.3	0	1.1
Export peak reduction	0	0	0	**0.4**
Arbitrage charge import	12.5	14.9	11.5	6.7
Arbitrage charge PV	6.3	**1.7**	6.3	**12.1**
Arbitrage discharge	19.5	17.8	20.0	20.4
Operation cost savings [1000 €]	34.0	**57.8**	**28.0**	**49.1**
Capacity cost savings [% of operation cost savings]	20.4	**60.0**	0	14.1
Energy cost savings [% of operation cost savings]	79.6	40.0	100	**85.9**
h_T [%]	72.0	71.4	72.7	70.8

  - During hours 3-6, 12, 15-17, 21 and 24, the prosumer imports without discharging or charging, so $v_t^{\text{sys}} = \pi_t^{\text{im}}$, as indicated by part (i) of Proposition 3.
  - In hours 7 and 20, the prosumer discharges and imports within the capacity limit, corresponding to parts (i) and (iv) of Proposition 3

- During hours 9-10, the net demand is negative and the prosumer exports within the network capacity without charging or discharging. Thus, the system price is equal to the export price, as per (ii) of Proposition 3.
- In hours 8, 11 and 18-19, the system price is between the import and export prices. The prosumer neither imports nor exports, but discharges in hours 8 and 18-19, while charges in hour 11, all within the PCS capacity. Thus, the BESS sets the system marginal cost, reflecting the degradation cost and the opportunity cost of the BESS.
- The system price is above the import price in hours 14 and 23. These two hours are similar in that the prosumer imports at the maximum network capacity due to high net demand. But in hour 14, the prosumer also charges at the maximum capacity and the SOC reaches the upper bound of 0.9, as the import price in this hour is relatively lower at 0.156 €/kWh. In hour 23, the prosumer discharges within the PCS capacity but the SOC reaches the lower bound. This is consistent with (i), (iii) and (iv) of Proposition 3.

We use hour 14 as an example to show how the marginal cost is calculated step by step. In this hour, the maximum capacity is reached. Based on Proposition 3 (i), a scarcity rent λ_t^{im} is generated, so $v_t^{\text{sys}} = \pi_t^{\text{im}} + \lambda_t^{\text{im}}$. In the simulation, $v_t^{\text{sys}} = 0.163$ €/kWh, which is the sum of $\pi_t^{\text{im}} = 0.156$ €/kWh and $\lambda_t^{\text{im}} = 0.007$ €/kWh.

We provide a detailed analysis of BESS operation status [2] and cost savings in Table 3. Case *A-70* reports results relative to a scenario without BESS. Although peak reduction occurs in only 1.3% of all hours, it accounts for 20.4% of the operation cost savings. Using the same PCS (57.8 kW) and battery capacity (122.6 kWh) as in case *A-70*, we evaluate three additional cases.

In case *A-70-HighCT*, the assumption on the day-ahead market clearing price remain the same as that in case *A-70*, but the network capacity tariff is increased from 1 to 5€/kW/month, while the volumetric network tariff is reduced from 0.05 €/kWh to 0.01 €/kWh for imports and to zero for exports. This is motivated by the fact that some DSOs, such as Fluvius Limburg in Belgium, impose network capacity tariffs as high as 5.67 EUR/kW/month. There are two notable observations. Firstly, the operation cost savings increase from 34.0 to 57.8 thousand €, with capacity cost savings representing 60%, implying the increased importance of targeting peak demand events under high network capacity

[2] "Not in operation": the BESS neither charges nor discharges, i.e., $p_t^{\text{ch}} = p_t^{\text{dis}} = 0$; "Import peak reduction": the BESS discharges and the import power reaches the network capacity, i.e., $p_t^{\text{dis}} > 0$ and $p_t^{\text{im}} = p_m^{\text{pk}}$; "Export peak reduction": the BESS charges and the export power reaches the network capacity, i.e., $p_t^{\text{ch}} > 0$ and $p_t^{\text{ex}} = p_m^{\text{pk}}$; "Arbitrage charge import": the BESS charges from imported power and import within network capacity, i.e., $p_t^{\text{ch}} > 0$ and $p_t^{\text{im}} > 0$ and $p_t^{\text{im}} < p_m^{\text{pk}}$; "Arbitrage charge PV": the BESS charges only from PV production and does not import, i.e., $p_t^{\text{ch}} > 0$ and $p_t^{\text{im}} = 0$; "Arbitrage discharge": arbitrage hours of discharging, i.e., $p_t^{\text{dis}} > 0$ and $p_t^{\text{im}} < p_m^{\text{pk}}$.

tariffs. Second, the share of hours in which the BESS charges from PV decreases, as direct export becomes more beneficial once the export tariff is eliminated. By contrast, in case *A-70-NoCT*, where the capacity tariff is removed, cost savings fall to 28 thousand €, reducing the economic attractiveness of BESS investment.

We further consider the *A-70-HighPV* case[3], where PV capacity increases from 80 kW to 400 kW while other parameters remain the same as case *A-70*. As shown in Table 3, the operation cost savings amount to 49.1 thousand €, much higher than in *A-70*. With abundant PV generation, the share of hours charging from PV rises from 6.3% to 12.1%, and 85.9% of the cost savings stem from energy arbitrage. This underscores the value of advanced algorithms that capture uncertainties in import / export prices and PV generation for such prosumers.

3.2.3. Scarcity rent

If either the import / export or charge / discharge reaches its limit in a certain hour, the scarcity rent is generated. We proceed to discuss how the scarcity rents recover the network capacity tariff, and the investment cost of the PCS and battery in Proposition 4.

Proposition 4. *When the constraints of the operation variables are active, the corresponding scarcity rent is generated, which covers the investment cost exactly. The following holds:*

(i) *The monthly procurement cost of network capacity is equal to accumulated scarcity rent from the import and export capacity limitations during the corresponding month, i.e.,* $\pi_m^{\mathrm{pk}} = \sum_{t\in\mathcal{T}_m} \lambda_t^{\mathrm{im}} + \sum_{t\in\mathcal{T}_m} \lambda_t^{\mathrm{ex}}$. *It can further be related to the system marginal cost and import / export prices* $\pi_m^{\mathrm{pk}} = \sum_{t\in\mathcal{T}_m,\ p_t^{\mathrm{im}}=p_m^{\mathrm{pk}}} (v_t^{\mathrm{sys}} - \pi_t^{\mathrm{im}}) + \sum_{t\in\mathcal{T}_m,\ p_t^{\mathrm{ex}}=p_m^{\mathrm{pk}}} (\pi_t^{\mathrm{ex}} - v_t^{\mathrm{sys}}), m \in \mathcal{M}_y, y \in \mathcal{Y}$.

(ii) *The investment cost of PCS is equal to the accumulated scarcity rent from charge and discharge limitations over the entire horizon, i.e.,* $C^{\mathrm{pcs}} = \sum_{t\in\mathcal{T}} \lambda_t^{\mathrm{ch}} + \sum_{t\in\mathcal{T}} \lambda_t^{\mathrm{dis}}$.

(iii) *The investment cost of the battery pack is equal to the accumulated scarcity rent from energy capacity limitations and the battery lifetime limitation , i.e.,*

$$C^{\mathrm{bat}} = (1 - h^{\dagger} - \sum_{t\in\mathcal{T}} \Delta h_t^{\mathrm{cal}}) \cdot \lambda_T^x - \sum_{t\in\mathcal{T}} \sum_{\tau\in\mathcal{T}_t} \Delta h_\tau^{\mathrm{cal}} \cdot (\overline{s} \cdot \overline{\lambda}_t^e - \underline{s} \cdot \underline{\lambda}_t^e) + \sum_{t\in\mathcal{T}} (\overline{s} - s_0) \cdot \overline{\lambda}_t^e + \sum_{t\in\mathcal{T}} (s_0 - \underline{s}) \cdot \underline{\lambda}_t^e.$$

It can be further broken down as follows:

- *In the first term, the sum* $\sum_{t\in\mathcal{T}} \Delta h_t^{\mathrm{cal}}$ *represents the accumulated calendar losses over the horizon. Since this degradation is not caused by BESS arbitrage, it is subtracted from the coefficient of* λ_T^x. *Additionally, the first term would be zero if the BESS does not reach the SOH threshold at the end of the investment horizon.*
- *The second term would be zero if* $\Delta h_\tau^{\mathrm{cal}} = 0$. *It therefore represents the lost opportunity cost due to calendar losses.*
- *The third term and the fourth term represent the accumulated scarcity rent due to energy capacity constraints* (5c) *and* (5d).

Regarding the monthly network capacity tariff, part (i) of Proposition 4 indicates both the scarcity rent from the import and export limitations contribute to it. However, in case *A-70*, λ_t^{ex} is always zero, and only 1.6% of all hours show positive values for λ_t^{im} (i.e., when the corresponding constraint is active regardless of charging or discharging), with the maximum values reaching 0.97. This is because the PV installation is relatively low due to the space limitation, and the prosumer mainly imports from the grid rather than export.

The investment cost of PCS amounts to 120 €/kW, and is recovered via $\sum_{t\in\mathcal{T}} \lambda_t^{\mathrm{ch}}$ and $\sum_{t\in\mathcal{T}} \lambda_t^{\mathrm{dis}}$ as described in (ii) of Proposition 4. In case *A-70*, the former sums to 12.7 €/kW with 4.1% of hours having positive values, while the latter sums to 107.3 €/kW, with 2.6% hours having positive values. This observation implies that although the BESS less frequently discharges at the maximum capacity, the value of λ_t^{dis} tends to be larger. This is because one important benefit of the BESS is to reduce the peak demand, which consequently lowers network capacity costs.

[3]This case simulates a large parking lot with 100 PV-covered spaces but only 20 equipped with charging posts, reflecting low EV penetration.

Table 4
Comparison of C^{bat} composition in case *A-70* with $h^{\dagger} = 70\%$ and a sensitivity with $h^{\dagger} = 75\%$ in case *A-75*, assuming an investment horizon of 10 years.

Case	*A-70*	*A-75*
$(1 - h^{\dagger} - \sum_{t\in\mathcal{T}} \Delta h_t^{\text{cal}}) \cdot \lambda_T^x$	0	26.58
$-\sum_{t\in\mathcal{T}} \sum_{\tau\in\mathcal{T}_t} \Delta h_\tau^{\text{cal}} \cdot (\overline{s} \cdot \overline{\lambda}_t^e - \underline{s} \cdot \underline{\lambda}_t^e)$	-8.85	-7.24
$\sum_{t\in\mathcal{T}} (\overline{s} - s_0) \cdot \overline{\lambda}_t^e + \sum_{t\in\mathcal{T}} (s_0 - \underline{s}) \cdot \underline{\lambda}_t^e$	158.85	130.66
Sum	150	150
h_T	72.0%	75.0%

Table 5
Breakdown of the *optimal* investment and operation status across various cases.

Cases	*A-70*	*A-70-HighCT*	*A-70-NoCT*	*A-70-HighPV*
Investment				
PCS [kW]	57.8	198.7	31.0	119.4
Battery [kWh]	122.6	469.2	90.1	424.6
Energy-to-power ratio	2.1	**2.4**	**2.9**	**3.6**
Status [% of all hours]				
Not in operation	60.4	44.2	60.2	41.0
Import peak reduction	1.3	**8.8**	0	2.5
Export peak reduction	0	0	0	1.4
Arbitrage charge import	12.5	23.1	13.8	8.4
Arbitrage charge PV	6.3	2.1	6.2	**15.7**
Arbitrage discharge	19.5	21.8	19.8	31.0
Operation cost savings [1000 €]	34.0	164.0	21.3	116.3
Network capacity cost savings [%]	20.4	62.0	0	11.8
Energy cost savings [%]	79.6	38.0	100	88.2
h_T [%]	72.0	73.3	72.8	76.6

Table 4 decomposes the battery investment cost $C^{\text{bat}} = 150$ €/kWh into three components for Cases *A-70* and *A-75*, directly illustrating (iii) of Proposition 4. The first term reflects the marginal value of battery durability. In Case *A-70*, $h_T = 72\% > h^{\dagger} = 70\%$, so the SOH constraint is inactive and $\lambda_T^x = 0$, making this term zero, therefore investing in a more durable battery with longer lifetime is not economically justified in this aspect. In Case *A-75*, the constraint binds at $h_T = h^{\dagger} = 75\%$, yielding $\lambda_T^x = 154.98$ €/kWh and a contribution of 26.58 €/kWh to C^{bat}. The second term represents the lost opportunity cost due to calendar losses. It is negative in both cases (-8.85 and -7.24 €/kWh), reflecting that passive calendar degradation reduces effective capacity over time. This passive degradation limits the energy available for future arbitrage and peak reduction, representing a foregone revenue stream that is not attributable to cycling. Consequently, the scarcity rents on energy capacity need not recover this passively lost capacity, which is why the second term is negative in both cases. The third and fourth terms are the accumulated scarcity rents from the upper and lower SOC bound constraints, and constitute the dominant component of battery cost recovery (158.85 €/kWh in*A-70*, 130.66 €/kWh in *A-75*). Battery degradation affects $\overline{\lambda}_t^e$ and $\underline{\lambda}_t^e$, thereby creating scarcity in battery energy capacity. The reduction from Case *A-70* to *A-75* occurs because the binding SOH constraint in Case *A-75* limits total cycling, reducing the frequency of SOC bound violations. All three components sum exactly to 150 €/kWh in both cases, confirming Proposition 4 (iii) and providing an internal consistency check of the numerical results.

We further compare the four cases discussed in Section 3.2, but here the BESS investments are optimized in each case rather than fixed as in *A-70*. The results are presented in Table 5. In *A-70-HighCT*, both PCS and battery investments increase, along with a higher energy-to-power ratio. This outcome is driven by two factors. First,

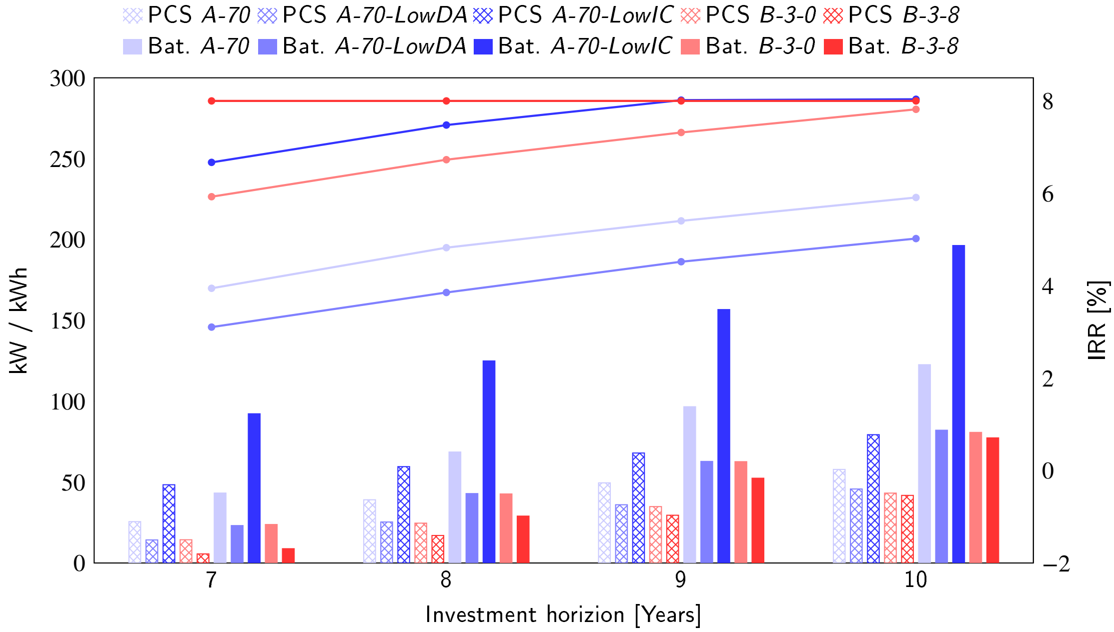

Figure 4: PCS (patched bars) and battery capacity, along with the ex-post calculated IRR (using the same color code for cases), for Cases *A-70*, *A-70-LowDA*, *A-70-LowIC*, *B-3-0*, and *B-3-8*

under a higher capacity tariff, prosumers have stronger incentives to reduce monthly peak demand, as reflected in the higher share of hours with import peak reduction standing at 8.8%. The resulting scarcity rents justify greater BESS investment. Second, since exports are exempt from volumetric tariffs, more opportunities for energy arbitrage arise, leading to a slightly higher energy-to-power ratio. In contrast, *A-70-NoCT* benefits only from energy arbitrage. Accordingly, both PCS and battery capacities decline, while the energy-to-power ratio increases. A more pronounced change occurs in *A-70-HighPV*, where BESS investment and, especially, the energy-to-power ratio rise substantially due to the need to absorb and arbitrage excess PV production. Overall, the comparison shows that higher capacity tariffs and greater PV generation both increase BESS investment by raising scarcity rents relative to the base case. However, when the main benefit stems from energy arbitrage, prosumers are better off adopting a larger energy-to-power ratio. It is also worth noting that Case *A-70-HighPV* exhibits a higher end-of-horizon SOH of 76.6% compared to the other cases. This attributes to the much larger energy-to-power ratio in this case, which results in shallower cycling per unit of capacity and therefore slower cycling-induced degradation over the 10-year horizon.

3.3. Impact of the IRR constraint on sizing

In the previous analysis of Propositions 2-4, we have ignored the discount factor and IRR constraint to better understand prosumer's behavior in investing and operating the BESS. In this section, we reintroduce the discount factor and IRR constraint to evaluate their impacts on the investment decisions. We first present Proposition 5 and then report simulation results based on the continuous model (1)–(6).

Proposition 5. *Let c denote the BESS investment cost, which is $C^{\mathrm{pcs}} \cdot x^{\mathrm{pcs}} + C^{\mathrm{bat}} \cdot x^{\mathrm{bat}}$ and let c_y represent the operation costs in year y, which is $\sum_{m\in\mathcal{M}_y} p^{\mathrm{pk}}_m \cdot \pi^{\mathrm{pk}}_m + \sum_{t\in\mathcal{T}_y}(p^{\mathrm{im}}_t \cdot \pi^{\mathrm{im}}_t - p^{\mathrm{ex}}_t \cdot \pi^{\mathrm{ex}}_t)$. The optimal value of c is denoted by $c^{\mathrm{irr},\star}$ and $c^\star$ for the case with and without IRR constraint, respectively. The following conditions hold:*

(i) If the IRR constraint (2) is not active even when explicitly imposed, then the BESS investment cost with and without the IRR constraint are the same $c^{\mathrm{irr},\star} = c^\star$.

(ii) If (2) is active and $\gamma^{\mathrm{irr}}_y < \gamma_y$, then the BESS investment cost with the IRR constraint will be less than the cost without the constraint $c^{\mathrm{irr},\star} < c^\star$.

Figure 4 shows the invested PCS and battery capacity as well as the ex-post calculated IRR, for investment horizons ranging from 7 to 10 years. We first compare case *B-3-0* without the IRR constraint and case *B-3-8* with an IRR requirement of 8%, as they are directly related to Proposition 5. We observe that as the investment horizon increases, the IRR of case *B-3-0* increases from 5.93% to 7.82%, which is primarily driven by more adequate utilization. This is because h_T has not reached $h^{\dagger}$ in all horizons, and a longer horizon allows for more adequate use of the BESS. Nevertheless, the resulting IRR remains below the 8% target. After explicitly imposing this requirement, we see a reduction in the invested capacity for both the battery and PCS. The difference in capacity is much smaller at the 10-year investment horizon, as the IRR of case *B-3-0* reaches 7.82%, which is close to the target. This case study demonstrates that if a prosumer needs financial support from a bank and needs a specific IRR to secure a loan, the prosumer may need to consider a longer investment horizon. Moreover, as implied by case *A-70-HighCT*, the high capacity tariff would increase the profitability of the BESS for the prosumer thereby reaching the IRR target.

We proceed to analyze several factors that impact the sizing and the realized IRR. By comparing Case *A-70* with Case *B-3-0*, we find that when the discount rate is not accounted for in the simulation, the model outputs over-invested results. The energy-to-power ratio also increases slightly, from 1.66–1.89 to 1.69–2.12, depending on the simulation horizon. This occurs because the model overestimates the value of future years, and consequently, the realized IRR after accounting for the discount factor is also much lower. Additional sensitivity analyses are conducted by reducing day-ahead market prices by 20% in Case *A-70-LowDA* and reducing the investment cost of the BESS by 20% in Case *A-70-LowIC*. The price spread decreases in Case *A-70-LowDA*, leading to lower investment and a lower realized IRR. In contrast, in Case *A-70-LowIC*, both investment and realized IRR increase significantly, reaching 8.04% for the 10-year investment horizon, indicating high sensitivity to the BESS investment costs.

In the current mathematical formulation, the investment horizon T is treated as an exogenous parameter. Making T endogenous would require binary variables indexing the terminal period, increasing computational complexity. However, the parametric analysis in Figure 4 substitutes for this because by comparing results across $T \in \{7, 8, 9, 10\}$ years, a prosumer can identify the minimum horizon required to meet a given IRR target. Take Case *B-3-8* as an instance, the 8% target remains infeasible within a 10-year horizon under the base tariff parameters, suggesting that prosumers seeking bank financing should either plan for a longer horizon or operate under high-capacity-tariff environments such as Case *A-70-HighCT*, where stronger scarcity rents improve profitability.

3.4. Impact of indivisibility on sizing and the economic loss

In Section 2.2, we have provided an upper bound for the economic loss caused by indivisibility. It serves as a valuable reference when the number of BESS models I is large or T is relatively small, (e.g., using representative days to represent a year). However, the analytical bound is loose for longer-horizon hourly models. We therefore directly estimate the indivisibility loss numerically by comparing the optimal objective values of the discrete model and the continuous model which provides a practically accurate assessment of the loss without relying on the analytical bound. More specifically, we conduct a numerical simulation to explore how the loss evolves with the scale of the prosumer. As shown in Figure 5, we scale the net demand curve, so that the peak ranges from 100 kW to 2000 kW. The orange curve shows the loss ranges from 2.1 to 154.9 € over the whole horizon, which is quite small in absolute terms. In relative terms, for a peak of 100 kW (invested PCS 8.4 kW and battery 15.5 kWh in the continuous model; 5 kW and 15 kWh in the discrete model), the cost saving from investing in the BESS is 865.4 €, and the relative saving amounts to a non-negligible 13.5%. But when the peak reaches 900 kW, even though the loss is the highest at 154.9 €, the relative value drops to 1.8%. Therefore, as the prosumer size increases, the loss becomes negligible, but under the condition that the available BESS energy and power capacity could be as low as 5 kW and 5 kWh respectively. This is further corroborated by the bar plots in Figure 5.

The bars in the figure show the capacity difference between the continuous and discrete model. In most cases, the investment resulting from the discrete model is smaller than that from the continuous model (negative bars). An interesting observation, contrary to intuition, is very notable in the 1000 kW simulation. The continuous model results in a capacity of 154.7 kW and 83.6 kWh, which is closer to the discrete solution of 155 kW and 85 kWh. However, the discrete model obtains 150 kW and 80 kWh, which is due to the IRR constraint.

4. Discussion

Theoretical analyses of BESS sizing and operation remain relatively scarce in the literature. Compared with [5], which analyzes scarcity rents for conventional generators, this study extends the framework to account for both power

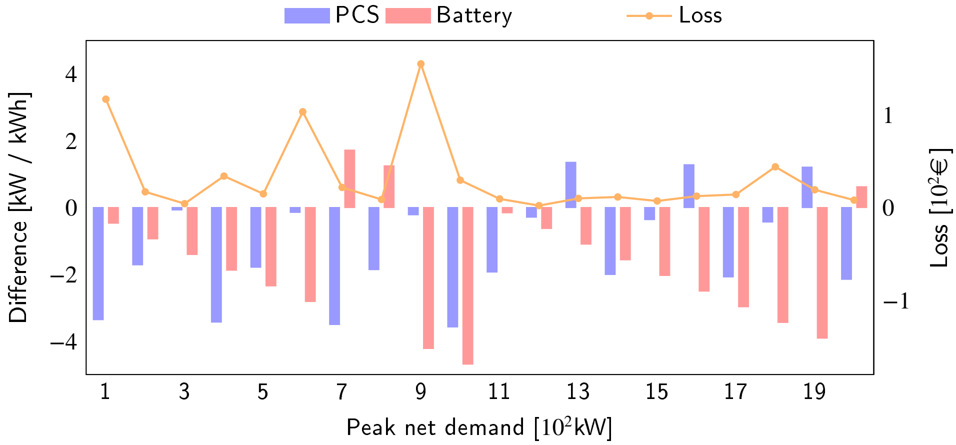

Figure 5: Difference in PCS and battery capacity (left y-axis) between cases *B-8-1* and *C-8-1*, along with the economic loss (right y-axis), with a 10-year investment horizon.

and energy capacity dimensions, as well as the impact of energy capacity degradation. Both [28] and [29] focus on storage and derive results analogous to our system marginal cost, but from a large power system perspective. Our work extends these results by considering a retail tariff structure that combines a volumetric charge based on kWh and a capacity charge based on peak kW, which is more representative of the prosumer context. Regarding IRR, most existing studies approach this topic through numerical simulation alone while our theoretical analysis in Proposition 5 provides a formal basis that is consistent with and explains the numerical findings of [31, 32, 33]. On indivisibility, prior analyses for conventional generators have been conducted for short-term economic dispatch [44] and long-term investment [45]. Our results are consistent with their structural findings in the sense that the duality gap is independent of the number of investment options under certain conditions, and we extend them to the prosumer BESS context.

The numerical results confirm and extend both the theoretical analysis and prior numerical studies. The dominance of energy arbitrage over peak reduction in the base case (79.6% vs. 20.4% of cost savings in Case *A-70*) is consistent with [33], which finds that energy cost savings are the primary driver of BESS profitability under volumetric tariffs. However, our results further show that this balance shifts substantially under higher capacity tariffs, because capacity savings rise to 62% in Case *A-70-HighCT*, which is theoretically grounded in Proposition 4 and has not been explicitly characterized in prior prosumer BESS studies. Regarding IRR, our finding that an 8% target requires a horizon of 10 years or longer under base tariff conditions is consistent with [31, 32], which report that BESS viability is highly sensitive to investment horizon and local tariff design, while Proposition 5 provides the formal theoretical basis for this sensitivity. On indivisibility, to our knowledge no prior prosumer BESS study has theoretically bounded or numerically quantified the efficiency loss from discrete BESS configurations. Our finding that the loss is negligible (below 2%) for prosumers with peak demand above 900 kW, but reaches 13.5% for small prosumers, has a direct practical implication that small prosumers should solve the discrete model explicitly, while large prosumers can rely on the continuous approximation.

5. Conclusions and future work

This paper examines BESS sizing and operation for prosumers under retail tariffs. Instead of modeling complex uncertainties in PV production, demand profiles, and future prices, we develop a comprehensive analysis framework where a continuous model is first presented in order to analyze sizing and operation principles through KKT analysis, supplemented by a discrete model to assess indivisibility losses. Various boundary conditions and prosumers' preference and characteristics are evaluated in the theoretical and numerical analysis. The study offers important insights into BESS sizing and operation for prosumers.

First, BESS and network capacity constraints generate scarcity rents that recover BESS investment costs and procured network capacity costs, respectively. BESS operation reflects complex interactions in which energy capacity constraints create opportunity costs, indirectly influenced by degradation. Second, higher capacity tariffs and abundant

Table 6
Actionable guidance on BESS sizing strategy.

Condition	Case	E/P ratio	Primary strategy
Base tariff	*A-70*	approx. 2.1 h	Mixed arbitrage and peak reduction
High capacity tariff	*A-70-HighCT*	approx. 2.4 h	Target peak demand hours
No capacity tariff	*A-70-NoCT*	approx. 2.9 h	Energy arbitrage only
High PV generation	*A-70-HighPV*	approx. 3.6 h	Maximise self-consumption

local PV generation provide stronger incentives for larger BESS investments. Under high capacity tariffs, prosumers should adopt a lower energy-to-power ratio and operate the BESS to target peak demand hours, as capacity charges may account for a major share of cost savings. By contrast, when benefits primarily stem from energy arbitrage, such as in cases of high PV generation or large import–export price spreads, prosumers should adopt a higher energy-to-power ratio and carefully account for uncertainties in prices and net demand. Third, at optimal investment, the end-of-life SOH threshold may not impose scarcity, in which case paying more for a longer-lasting battery is not economically justified. Meeting IRR targets may require reduced investments, at the cost of lower total savings, but lower BESS investment costs can make the target easier to achieve. In contrast, network capacity tariffs can significantly enhance BESS profitability. On the other hand, policymakers may consider implementing capacity charge in the retail tariff to incentivize BESS investment if the price spreads are not attractive. Finally, directly adopting the nearest PCS and battery models from the continuous solution may not be optimal, demonstrating the necessity of a discrete model.

Table 6 summarizes actionable guidance on energy-to-power ratio selection and BESS operation strategy for prosumers under different tariff and load conditions. While the exact figures are case-specific, the directional trends are broadly advisory. Three practical recommendations follow. First, prosumers facing high network capacity tariffs should adopt a lower energy-to-power ratio and size the PCS generously relative to the battery, since the dominant value driver is peak demand reduction rather than energy throughput. Second, prosumers with abundant PV generation or large import–export price spreads should adopt a higher energy-to-power ratio to maximise arbitrage value, and should invest in uncertainty-aware forecasting tools given the sensitivity of arbitrage revenue to price and generation uncertainty. Third, when capacity tariffs are absent, the overall profitability of BESS investment declines substantially as cost savings fall from 34 thousand € to 21.3 thousand € in Cases *A-70* vs. *A-70-NoCT* at optimal investment, and prosumers should carefully assess whether energy arbitrage alone justifies the investment given their IRR requirements.

Some limitations of the proposed model and directions for future work are as follows. A primary direction for future work is to quantify the expected value of perfect information (EVPI) for prosumer BESS decisions by comparing the perfect-foresight benchmark derived from our framework against practical uncertainty-aware approaches [39, 46]. This would involve constructing a scenario set representing uncertainty in day-ahead prices, PV generation, and BESS costs; solving a stochastic or robust counterpart of the sizing and operation problem over these scenarios; and evaluating both the perfect-foresight and stochastic solutions on the same out-of-sample realizations to measure the gap.

Second, the degradation model could be enhanced beyond current linear assumptions for the cycling loss or an ex-post evaluation could be conducted to assess how sensitive the investment decisions are to this linearity assumption. For instance, battery degradation typically accelerates at high depths of discharge or elevated C-rates, then the temporal distribution of scarcity rents would change relative to the linear case. Specifically, hours with deep cycling would incur higher degradation costs, raising the system marginal cost during those periods and potentially shifting the optimal capacity split toward a larger battery relative to the PCS, i.e., a higher energy-to-power ratio. Quantifying this effect would require a non-linear degradation model, at the cost of losing the convexity that enables the KKT analysis.

Third, the numerical simulations suggest potential for tighter theoretical bounds on indivisibility losses. Since BESS techno-economic parameters vary across providers, comprehensive datasets could further validate the discrete model. The numerical simulations in this study are based on a single EV charging station, which may limit the direct transferability of quantitative findings. Future work should apply the proposed framework to a broader range of prosumer types, to assess how load profile characteristics affect optimal BESS sizing and the relative importance of peak reduction versus energy arbitrage.

The model might also be extended to utility-scale BESS providing auxiliary services in various electricity markets. Beyond the directions already discussed, future work could explore multi-prosumer settings where several co-located prosumers share BESS infrastructure, raising questions of cost allocation and cooperative investment. The framework could also be extended to incorporate time-varying BESS costs to capture the impact of continued cost reductions on optimal investment timing. Finally, as regulators increasingly consider dynamic network tariffs [47], extending the model to time-varying capacity charges would further improve its policy relevance.

CRediT authorship contribution statement

Yuting Mou: Conceptualization, Methodology, Software, Formal analysis, Investigation, Data Curation, Writing - Original Draft, Writing - Review & Editing, Visualization, Funding acquisition.

Declaration

During the preparation of this work the author used ChatGPT in order to correct language errors. After using this tool, the author reviewed and edited the content as needed and takes full responsibility for the content of the publication.

Acknowledgment

The work is supported by the National Natural Science Foundation of China (Grant No. 62403126). We sincerely thank the editor and reviewers for their valuable and constructive suggestions.

Appendix

A. Integrated investment-operation model for conventional generators

A stylized integrated investment-operation model which only involves the energy market can be formulated as follows.

$$\min_{x,p} \sum_{i\in\mathcal{I}} IC_i \cdot x_i + \sum_{t\in\mathcal{T}} \sum_{i\in\mathcal{I}} MC_i \cdot p_{i,t} \tag{10a}$$

$$\text{s.t. } p_{i,t} - x_i \leq 0, i \in \mathcal{I}, t \in \mathcal{T} \qquad (\mu_{i,t}) \tag{10b}$$

$$D_t - \sum_{i\in\mathcal{I}} p_{i,t} = 0, t \in \mathcal{T} \qquad (\lambda_t) \tag{10c}$$

$$x, p \geq 0 \tag{10d}$$

We represent time periods as $t \in \mathcal{T}$ and technologies as $i \in \mathcal{I}$. The investment cost and marginal cost of technology i are denoted as IC_i and MC_i, respectively. The invested capacity of technology i is represented by x_i. The production of technology i to meet demand in period t is represented by $p_{i,t}$ and it is limited by x_i, as shown in equation (10b). The demand for electricity in period t is represented by D_t, and the power balance is given by equation (10c). The KKT conditions of this model can be described as follows:

$$0 \leq \mu_{i,t} \perp x_i - p_{i,t} \geq 0, i \in \mathcal{I}, t \in \mathcal{T} \tag{11a}$$

$$0 \leq p_{i,t} \perp MC_i + \mu_{i,t} - \lambda_t \geq 0, i \in \mathcal{I}, t \in \mathcal{T} \tag{11b}$$

$$0 \leq x_i \perp IC_i - \sum_{t\in\mathcal{T}} \mu_{i,t} \geq 0, i \in \mathcal{I} \tag{11c}$$

where λ_t is interpreted as the equilibrium energy price for period t, and $\mu_{i,t}$ is the scarcity rent of technology in period, i.e., the earnings of the technology above its marginal cost.

Starting from (11b), if $p_{i,t} > 0$, it implies that technology i is actively producing during period t. In this case, we have $MC_i + \mu_{i,t} - \lambda_t = 0$, which means the scarcity rent $\mu_{i,t}$ is exactly the short-term profit at period t from the energy market, i.e., $\mu_{i,t} = \lambda_t - MC_i$. Moving on to (11c), if we decide to invest in technology i ($x_i > 0$), we have $IC_i - \sum_{t\in\mathcal{T}} \mu_{i,t} = 0$. This indicates the short-term profit over the entire horizon should cover the investment cost if we choose to invest in technology i. In other words, if net present value (NPV) is positive, we increase the investment until it reaches zero. However, if NPV turns out to be negative, implying $IC_i - \sum_{t\in\mathcal{T}} \mu_{i,t} > 0$, the complementary condition (11c) suggests investment x_i must be zero. Thus, we do not invest in technology i.

B. Proofs

B.1. Proof of Proposition 1

Various methods have been proposed to bound the duality gap of separable nonconvex problems, such as the Shapley-Folkman theorem [48, 49] or other methods relying on basic linear programming theory [50]. Suppose both Problem (8) and its relaxation are feasible, and we follow the reasoning of references [45, 50] to upper bound the indivisibility loss.

To create a separable structure, we divide p_m^{pk}, p_t^{im} and p_t^{ex} into I parts, so that each BESS i is associated with a $p_{i,m}^{\mathrm{pk}}$, $p_{i,t}^{\mathrm{im}}$ and $p_{i,t}^{\mathrm{ex}}$. Constraints (8d) and (8e) could be modified accordingly, and together with constraints (8f)-(8o), we define the operation set of BESS i, denoted as $\mathcal{Z}_i$. In the relaxation of Problem (8), the decision variables related to BESS i, denoted by $\mathbf{z}_i$, can be represented as a linear combination of the extreme points of $\mathcal{Z}_i$, i.e. $\mathbf{z}_i = \sum_{k\in\mathcal{K}_i} \theta_{i,k} \cdot \hat{\mathbf{z}}_{i,k}$, where the set $\mathcal{K}_i$ denotes the indices of extreme points of $\mathcal{Z}_i$ and $\hat{\mathbf{z}}_{i,k}$ represents the k-th extreme point. Problem (12) can then be formulated with $\theta_{i,k}$ as the optimization variable, which is equivalent to the relaxation of Problem (8).

$$\min_{\theta_{i,k}} \sum_{i\in\mathcal{I}} \sum_{k\in\mathcal{K}_i} \theta_{i,k} \cdot \Big(C_i^{\mathrm{es}} \cdot \hat{u}_{i,k} + \sum_{y\in\mathcal{Y}} \big(\sum_{m\in\mathcal{M}_y} \hat{p}_{i,m,k}^{\mathrm{pk}} \cdot \pi_m^{\mathrm{pk}} + \sum_{t\in\mathcal{T}_y} (\hat{p}_{i,t,k}^{\mathrm{im}} \cdot \pi_{i,t,k}^{\mathrm{im}} - \hat{p}_{i,t,k}^{\mathrm{ex}} \cdot \pi_t^{\mathrm{ex}}) \big) \cdot \gamma_y \Big) \tag{12a}$$

$$\begin{aligned} \text{s.t.} \sum_{i\in\mathcal{I}} \sum_{k\in\mathcal{K}_i} \theta_{i,k} \cdot C_i^{\mathrm{es}} \cdot \hat{u}_{i,k} - \sum_{y\in\mathcal{Y}} \Big(C_y \\ - \sum_{k\in\mathcal{K}_i} \theta_{i,k} \cdot \big(\sum_{m\in\mathcal{M}_y} \hat{p}_{i,m,k}^{\mathrm{pk}} \cdot \pi_m^{\mathrm{pk}} + \sum_{t\in\mathcal{T}_y} (\hat{p}_{i,t,k}^{\mathrm{im}} \cdot \pi_{i,t,k}^{\mathrm{im}} - \hat{p}_{i,t,k}^{\mathrm{ex}} \cdot \pi_t^{\mathrm{ex}}) \big) \Big) \cdot \gamma_y^{\mathrm{irr}} \le 0 \end{aligned} \tag{12b}$$

$$\sum_{i\in\mathcal{I}} \sum_{k\in\mathcal{K}_i} \theta_{i,k} \cdot (\hat{p}_{i,t}^{\mathrm{dis}} - \hat{p}_{i,t}^{\mathrm{ch}} + \hat{p}_{i,t}^{\mathrm{im}} - \hat{p}_{i,t}^{\mathrm{ex}}) = D_t^{\mathrm{net}}, t \in \mathcal{T} \tag{12c}$$

$$\sum_{k\in\mathcal{K}_i} \theta_{i,k} = 1, i \in \mathcal{I} \tag{12d}$$

$$\theta_{i,k} \ge 0, i \in \mathcal{I}, k \in \mathcal{K}_i \tag{12e}$$

For each BESS model i, there are K_i variables $\theta_{i,k}$. From constraint (12d), there is at least one non-zero $\theta_{i,k}$ per BESS i. If there is exactly one for each i, $\sum_{k\in\mathcal{K}_i} \theta_{i,k} \cdot \hat{u}_{i,k}$ would be binary, making the solution of Problem (12) feasible for Problem (8).

Suppose the number of BESS models I is larger than $T+1$. From the fundamental theorem of linear programming theory, there is an optimal solution that has at least as many constraints as variables that are tight. Therefore, it follows there are at most $T + 1$ (the number of constraints in (12b)-(12c)) additional non-zero $\theta_{i,k}$. In other words, if these constraints are tight, for some $\theta_{i,k}$, constraint (12e) does not need to be tight, so these $\theta_{i,k}$ could be non-zero. This implies at most $T + 1$ BESS models have more than one $\theta_{i,k} > 0$, which makes the solution infeasible for Problem (8). Starting from the BESS that solves Problem (12), at most $T + 1$ should be modified to obtain a feasible solution to Problem (8). The modification costs ρ, which is the maximum cost resulting from converting an infeasible $\sum_{k\in\mathcal{K}_g} \theta_{i,k} \cdot \hat{\mathbf{z}}_{i,k} \in \mathrm{conv}(\mathcal{Z}_i)$ to a feasible one that supplies at least as much power by discharging or importing. We conclude that $IL \le \rho \cdot (T + 1)$. This conclusion indicates that the bound on the indivisibility loss is independent of the number of BESS models if I is larger than $T + 1$.

The analytical bound is most useful when T is small, such as in representative-day models ($T = 24$ or 96), where it provides a meaningful guarantee on indivisibility losses without solving the MILP. For longer-horizon hourly models, the bound becomes too loose to be practically informative, and direct numerical evaluation of IL via comparison of Problems (8) and its linear relaxation is more appropriate.

The modification cost ρ represents the maximum cost of converting a fractional BESS solution, which is a convex combination of discrete configurations from the linear relaxation, into a feasible discrete solution that supplies at least as much power. It encompasses two sources of economic loss, i.e., (i) capital mismatch arising from rounding up to a discrete available module size; and (ii) operational mismatch arising when the nearest feasible discrete configuration is smaller than the continuous optimum, restricting the feasible operating region and preventing the prosumer from replicating the optimal charging and discharging schedule, thereby increasing operational costs by importing from or exporting to the grid sub-optimally. To illustrate, suppose the continuous optimum requires a PCS of 8.5 kW and a battery of 17 kWh, but the available discrete options are 5 kW/10 kWh and 10 kW/20 kWh. Rounding up to 10 kW/20 kWh incurs capital overspend but preserves or improves operational performance due to the larger feasible region. Rounding down to 5 kW/10 kWh avoids capital overspend but restricts charging and discharging decisions, potentially missing peak reduction or arbitrage opportunities and thus increasing net operational costs. The parameter ρ upper-bounds the worst-case combined loss across all such rounding decisions over all BESS models $i \in \mathcal{I}$.

B.2. Proof of Proposition 2

Equations (4a) and (4b) imply that $x^{\text{bat}}_{t-1} > x^{\text{bat}}_{t}$. Since $h^{\dagger} \cdot x^{\text{bat}} - x^{\text{bat}}_{T} \leq 0$, we also have $h^{\dagger} \cdot x^{\text{bat}} - x^{\text{bat}}_{t} > 0$ for $t < T$. Based on the complementary slackness condition in (7q), the associated Lagrange multiplier λ^{x}_{t} is zero when the constraint is inactive. Therefore part (i) holds. This result indicates that the end-of-life SOH constraint can only become active at the end of the investment horizon because the calendar loss always exists.

From (7j) and (7k), we have

$$-\nu^{e}_{t} + \nu^{e}_{t+1} + \overline{\lambda}^{e}_{t} - \underline{\lambda}^{e}_{t} = 0, t < T,$$

$$-\nu^{e}_{T} + \overline{\lambda}^{e}_{T} - \underline{\lambda}^{e}_{T} = 0.$$

Summing over $t \in \mathcal{T}$ yields:

$$\sum\nolimits_{t=1}^{T-1} (-\nu^{e}_{t} + \nu^{e}_{t+1} + \overline{\lambda}^{e}_{t} - \underline{\lambda}^{e}_{t}) + (-\nu^{e}_{T} + \overline{\lambda}^{e}_{T} - \underline{\lambda}^{e}_{T}) = 0,$$

implying $\nu^{e}_{1} = \sum_{t\in\mathcal{T}} (\overline{\lambda}^{e}_{t} - \underline{\lambda}^{e}_{t})$. Furthermore, by recursive substitution:

$$\nu^{e}_{t} = \nu^{e}_{t-1} + \underline{\lambda}^{e}_{t-1} - \overline{\lambda}^{e}_{t-1} = \ldots = \nu^{e}_{1} + \sum\nolimits_{\tau=1}^{t-1} (\underline{\lambda}^{e}_{\tau} - \overline{\lambda}^{e}_{\tau}).$$

Substituting the expression for ν^{e}_{1}, we obtain:

$$\nu^{e}_{t} = \sum\nolimits_{\tau=t}^{T} (\overline{\lambda}^{e}_{\tau} - \underline{\lambda}^{e}_{\tau}),$$

and thus (ii) holds.

Similarly, we derive

$$\nu^{x}_{1} = \sum\nolimits_{t\in\mathcal{T}} (-\overline{s} \cdot \overline{\lambda}^{e}_{t} + \underline{s} \cdot \underline{\lambda}^{e}_{t} - \lambda^{x}_{t}),$$

$$\nu^{x}_{t} = \nu^{x}_{1} + \sum\nolimits_{\tau=1}^{t-1} (\overline{s} \cdot \overline{\lambda}^{e}_{\tau} - \underline{s} \cdot \underline{\lambda}^{e}_{\tau} + \lambda^{x}_{\tau}).$$

Since $\lambda^{x}_{t} = 0$ for $t < T$, part (iii) follows directly.

B.3. Proof of Proposition 3

From the perspective of power exchange with the main grid, in part (i), for $0 < p^{\text{im}}_{t} < p^{\text{pk}}_{m}$ and from (7o), we obtain $\lambda^{\text{im}}_{t} = 0$. This implies that the import power is within the procured network capacity limit and the network capacity is not in a state of scarcity. Further, from (7d), we conclude $\nu^{\text{sys}}_{t} = \pi^{\text{im}}_{t} + \lambda^{\text{im}}_{t} = \pi^{\text{im}}_{t}$. In contrast, if the import capacity constraint binds, λ^{im}_{t} represents the scarcity rent[4], given by $\nu^{\text{sys}}_{t} - \pi^{\text{im}}_{t}$. This means that, due to the scarcity of network capacity, the prosumer cannot import enough power to bring the system marginal cost down to the import price. Part (ii) follows the same reasoning.

When the prosumer is neither importing nor exporting, or is importing / exporting at the maximum capacity, the system marginal cost cannot be directly determined from the import / export status. Instead, it is clearer to evaluate it from the perspective of the opportunity and degradation costs of the BESS. In part (iii), for $0 < p^{\text{ch}}_{t} < x^{\text{pcs}}$ and from (7m), we obtain $\lambda^{\text{ch}}_{t} = 0$. Furthermore, from (7f) we have $\nu^{\text{sys}}_{t} = -\lambda^{\text{ch}}_{t} + \alpha \cdot \nu^{x}_{t} - \eta^{\text{ch}} \cdot \nu^{e}_{t} = \alpha \cdot \nu^{x}_{t} - \eta^{\text{ch}} \cdot \nu^{e}_{t}$. Substituting the expressions for ν^{x}_{t} and ν^{e}_{t} based on Proposition 2, part (iii) holds. Part (iv) follows similarly.

[4]This term is borrowed from power system economics [51], where it is used to describe the profit that a low marginal cost producer makes when the market clearing price exceeds its marginal cost. The market clearing price is analogous to the system marginal cost of the prosumer in this study.

B.4. Proof of Proposition 4

From (7d) and (7e), the scarcity rent of the network capacity is the difference between the system marginal cost and the import / export price, i.e., $\lambda_t^{\mathrm{im}} = \nu_t^{\mathrm{sys}} - \pi_t^{\mathrm{im}}$ and $\lambda_t^{\mathrm{ex}} = \pi_t^{\mathrm{ex}} - \nu_t^{\mathrm{sys}}$. Due to the complementary slackness conditions of (7c), since p_m^{pk} is non-zero, $\forall m \in \mathcal{M}_y, y \in \mathcal{Y}$, we have

$$\begin{aligned} \pi_m^{\mathrm{pk}} &= \sum_{t\in\mathcal{T}_m} \lambda_t^{\mathrm{im}} + \sum_{t\in\mathcal{T}_m} \lambda_t^{\mathrm{ex}} \\ &= \sum_{t\in\mathcal{T}_m,\ p_t^{\mathrm{im}}=p_m^{\mathrm{pk}}} (\nu_t^{\mathrm{sys}} - \pi_t^{\mathrm{im}}) + \sum_{t\in\mathcal{T}_m,\ p_t^{\mathrm{ex}}=p_m^{\mathrm{pk}}} (\pi_t^{\mathrm{ex}} - \nu_t^{\mathrm{sys}}). \end{aligned}$$

Part (ii) follows the same reasoning.

Due to the complementary slackness conditions of (7b), since $x^{\mathrm{bat}} > 0$, we have $C^{\mathrm{bat}} = -\sum_{t\in\mathcal{T}} \lambda_t^x \cdot h^\dagger + \sum_{t\in\mathcal{T}} \nu_t^x \cdot \Delta h_t^{\mathrm{cal}} - \nu_1^x - s_0 \cdot \nu_1^e$. Substituting the expressions for ν_t^x, ν_1^x and ν_1^e based on Proposition 2, we get

$$\begin{aligned} C^{\mathrm{bat}} &= -\sum_{t\in\mathcal{T}} \lambda_t^x \cdot h^\dagger + \sum_{t\in\mathcal{T}} \nu_t^x \cdot \Delta h_t^{\mathrm{cal}} - \sum_{t\in\mathcal{T}} (-\overline{s} \cdot \overline{\lambda}_t^e + \underline{s} \cdot \underline{\lambda}_t^e - \lambda_t^x) - s_0 \cdot \sum_{t\in\mathcal{T}} (\overline{\lambda}_t^e - \underline{\lambda}_t^e) \\ &= (1 - \sum_{t\in\mathcal{T}} \Delta h_t^{\mathrm{cal}} - h^\dagger) \cdot \sum_{t\in\mathcal{T}} \lambda_t^x - \sum_{t\in\mathcal{T}} \sum_{\tau=t}^{T} \Delta h_t^{\mathrm{cal}} \cdot (\overline{s} \cdot \overline{\lambda}_\tau^e - \underline{s} \cdot \underline{\lambda}_\tau^e) + \sum_{t\in\mathcal{T}} (\overline{s} - s_0) \cdot \overline{\lambda}_t^e + \sum_{t\in\mathcal{T}} (s_0 - \underline{s}) \cdot \underline{\lambda}_t^e \\ &= (1 - h^\dagger - \sum_{t\in\mathcal{T}} \Delta h_t^{\mathrm{cal}}) \cdot \lambda_T^x - \sum_{t\in\mathcal{T}} \sum_{\tau\in\mathcal{T}_t} \Delta h_\tau^{\mathrm{cal}} \cdot (\overline{s} \cdot \overline{\lambda}_t^e - \underline{s} \cdot \underline{\lambda}_t^e) + \sum_{t\in\mathcal{T}} (\overline{s} - s_0) \cdot \overline{\lambda}_t^e + \sum_{t\in\mathcal{T}} (s_0 - \underline{s}) \cdot \underline{\lambda}_t^e. \end{aligned}$$

Therefore, part (iii) is established.

B.5. Proof of Proposition 5

In part (i), if (2) not active, the models with and without the IRR constraint are equivalent, so $c^{\mathrm{irr},\star} = c^\star$.

For part (ii), when the IRR constraint is active, we consider relaxing it. Let $\lambda^\star$ be the optimal multiplier associated with (2), and considering C_y, the operation costs without BESS, is a constant. After relaxing (2), we rewrite the objective function of Problem (1)–(6) as:

$$\begin{aligned} & c - \textstyle\sum_{y\in\mathcal{Y}} (C_y - c_y) \cdot \gamma_y + \lambda^\star \cdot \left(c - \textstyle\sum_{y\in\mathcal{Y}} (C_y - c_y) \cdot \gamma_y^{\mathrm{irr}}\right) \\ =& (1 + \lambda^\star) \cdot c - \textstyle\sum_{y\in\mathcal{Y}} (1 + \gamma_y^{\mathrm{irr}}/\gamma_y \cdot \lambda^\star) \cdot (C_y - c_y) \cdot \gamma_y. \end{aligned}$$

Here c represents the BESS investment cost, and $(C_y - c_y) \cdot \gamma_y$ reflects the cost saving from investing the BESS. The effect of (2) is equivalent to increasing the investment cost by a factor of $1+\lambda^\star$, while the cost saving are increased by a factor of $1+\gamma_y^{\mathrm{irr}}/\gamma_y \cdot \lambda^\star$ for each year y. Since typically $\gamma_y^{\mathrm{irr}}/\gamma_y < 1$, the saving increases less than the cost. Therefore, to meet the IRR constraint, the prosumer will have to reduce the investment cost in exchange of less reduced cost saving. In the case where $\gamma_y^{\mathrm{irr}}/\gamma_y \geq 1$, which is not practical, the IRR constraint would be automatically satisfied. This can be verified by comparing the objective (1) and the IRR constraint (2).

C. Nomenclature

The dual variables are already associated with the constraints of the continuous model (1)–(6) and omitted here.

C.1. Index and sets

$y \in \mathcal{Y}$	Set of years
$m \in \mathcal{M}$	Set of months
$t \in \mathcal{T}$	Set of time steps, from 1 to T
$\tau \in \mathcal{T}_t$	Set of time steps, from 1 to t
$\mathcal{T}_y$	Set of time steps belonging to year $y \in \mathcal{Y}$
$\mathcal{M}_y$	Set of months belonging to year $y \in \mathcal{Y}$
$i \in \mathcal{I}$	Set of different BESS models

C.2. Parameters

C^{pcs} Overnight investment cost of PCS [€/kW]

C^{bat} Overnight investment cost of the battery [€/kWh]

η^{dis} Discharging efficiency

η^{ch} Charging efficiency

π_t^{im} Import price of electricity [€/kWh]

π_t^{ex} Export price of electricity [€/kWh]

π^{pk} Network capacity tariff [€/kW/month]

D_t^{net} Net demand at time step t [kW]

γ^{irr} Target internal rate of return

r Discount rate

s_0 Initial state of charge

C_y Total operation cost in year y without BESS [€]

$h^{\dagger}$ Minimum state of heath at the end of the lifetime

$\overline{s}$ Maximum allowed state of charge of the BESS

$\underline{s}$ Minimum allowed state of charge of the BESS

$\Delta h_t^{\mathrm{cal}}$ Calendar loss during the interval $t-1$ to t

α Coefficient for cycling loss

C_i^{es} Overnight investment cost of BESS model i [€]

$p_i^{\diamond}$ Rated power capacity of the BESS model i [kW]

$x_i^{\diamond}$ Rated energy capacity of the BESS model i [kWh]

C.3. Variables

x^{pcs} Invested power capacity of the PCS [kW]

x^{bat} Invested energy capacity of the battery [kWh]

x_t^{bat} Energy capacity of the battery pack at t [kWh]

p_t^{ch} Charging power at t [kW]

p_t^{dis} Discharging power at t [kW]

p_t^{ex} Export power at t [kW]

p_t^{im} Import power at t [kW]

p_m^{pk} Procured network capacity in month m [kW]

e_t Remaining energy in the battery at t

u_i Binary to indicate whether BESS model i is invested

$\theta_{i,k}$ Used for non-negative linear combination

References

[1] European Commission. Clean energy for all Europeans package, 2019.

[2] Saied Dardour, Deborah Ayres, and Lourdes Zamora. Renewable power generation costs in 2024. Technical report, International Renewable Energy Agency, 2025.

[3] Arizona Public Service. Rate schedule r-3 residential service time-of-use 4pm to 7pm weekdays with demand charge, 2025.

[4] Yikang Xiao, Yuting Mou, Bo Pan, and Min Yang. The design of a time-of-use tariff with a demand charge for residential electric vehicle charging posts. *Utilities Policy*, 97:102078, 2025.

[5] Yuting Mou, Anthony Papavasiliou, Katharina Hartz, Alexander Dusolt, and Christian Redl. An analysis of shortage pricing and capacity remuneration mechanisms on the pan-European common energy market. *Energy Policy*, 183:113843, 2023.

[6] Todd Levin, John Bistline, Ramteen Sioshansi, Wesley J. Cole, Jonghwan Kwon, Scott P. Burger, George W. Crabtree, Jesse D. Jenkins, Sonja Wogrin, and Benjamin F. Hobbs. Energy storage solutions to decarbonize electricity through enhanced capacity expansion modelling. *Nature Energy*, 8(11):1199–1208, 2023.

[7] Timm Weitzel and Christoph H. Glock. Energy management for stationary electric energy storage systems: A systematic literature review. *European Journal of Operational Research*, 264(2):582–606, 2018.

[8] Ali Ehsan and Qiang Yang. Coordinated investment planning of distributed multi-type stochastic generation and battery storage in active distribution networks. *IEEE Transactions on Sustainable Energy*, 10(4):1813–1822, 2019.

[9] Rahul Gupta and Fabrizio Sossan. Optimal sizing and siting of energy storage systems considering curtailable photovoltaic generation in power distribution networks. *Applied Energy*, 339:120955, 2023.

[10] Joseph J. Kelly and Paul G. Leahy. Sizing battery energy storage systems: Using multi-objective optimization to overcome the investment scale problem of annual worth. *IEEE Transactions on Sustainable Energy*, 11(4):2305–2314, 2020.

[11] Tiong Teck Teo, Logenthiran Thillainathan, Wai Lok Woo, and Khalid Abidi. Intelligent controller for energy storage system in grid-connected microgrid. *IEEE Transactions on Systems, Man, and Cybernetics: Systems*, 51(1):650–658, 2021.

[12] Mohammad Mehdi Hosseini and Masood Parvania. Hierarchical intelligent operation of energy storage systems in power distribution grids. *IEEE Transactions on Sustainable Energy*, 14(2):741–750, 2023.

[13] Per Aaslid, Magnus Korpås, Michael M Belsnes, and Olav B Fosso. Stochastic optimization of microgrid operation with renewable generation and energy storages. *IEEE Transactions on Sustainable Energy*, 13(3):1481–1491, 2022.

[14] Ye Tang, Qiaozhu Zhai, and Jiexing Zhao. Multi-stage robust economic dispatch with virtual energy storage and renewables based on a single level model. *IEEE Transactions on Automation Science and Engineering*, 21(4):5490–5502, 2024.

[15] Yonghui Sun, Xiaopeng Wu, Jianxi Wang, Dongchen Hou, and Sen Wang. Power compensation of network losses in a microgrid with bess by distributed consensus algorithm. *IEEE Transactions on Systems, Man, and Cybernetics: Systems*, 51(4):2091–2100, 2021.

[16] Jason Martins and John Miles. A techno-economic assessment of battery business models in the UK electricity market. *Energy Policy*, 148:111938, 2021.

[17] Thomas Mercier, Mathieu Olivier, and Emmanuel De Jaeger. The value of electricity storage arbitrage on day-ahead markets across Europe. *Energy Economics*, 123:106721, 2023.

[18] A. Belmondo Bianchi, H.H.M. Rijnaarts, and S. Shariat Torbaghan. Uncertainty-aware energy storage investment planning through arbitrage in DA and RT markets using novel block orders. *Journal of Energy Storage*, 110:115197, 2025.

[19] Joseph.J. Kelly and Paul.G. Leahy. Optimal investment timing and sizing for battery energy storage systems. *Journal of Energy Storage*, 28:101272, 2020.

[20] Saeed Ghadimi and Warren B. Powell. Stochastic search for a parametric cost function approximation: Energy storage with rolling forecasts. *European Journal of Operational Research*, 312(2):641–652, 2024.

[21] Makedon Karasavvidis, Dimitrios Papadaskalopoulos, and Goran Strbac. Optimal offering of energy storage in electricity markets with loop blocks. *IEEE Transactions on Power Systems*, 39(1):299–315, 2024.

[22] Gilles Bertrand and Anthony Papavasiliou. Adaptive trading in continuous intraday electricity markets for a storage unit. *IEEE Transactions on Power Systems*, 35(3):2339–2350, 2020.

[23] Paul Johnson, Dávid Zoltán Szabó, and Peter Duck. Optimal trading with regime switching: Numerical and analytic techniques applied to valuing storage in an electricity balancing market. *European Journal of Operational Research*, 319(2):611–624, 2024.

[24] Benedikt Finnah, Jochen Gönsch, and Florian Ziel. Integrated day-ahead and intraday self-schedule bidding for energy storage systems using approximate dynamic programming. *European Journal of Operational Research*, 301(2):726–746, 2022.

[25] Ehsan Nasrolahpour, Jalal Kazempour, Hamidreza Zareipour, and William D. Rosehart. A bilevel model for participation of a storage system in energy and reserve markets. *IEEE Transactions on Sustainable Energy*, 9(2):582–598, 2018.

[26] Dirk Lauinger, François Vuille, and Daniel Kuhn. Frequency regulation with storage: On losses and profits. *European Journal of Operational Research*, 319(2):442–455, 2024.

[27] Virginia Casella, Alice La Fata, Stefano Suzzi, Giulia Barbero, and Riccardo Barilli. The United Kingdom electricity market mechanism: A tool for a battery energy storage system optimal dispatching. *Renewable Energy*, 231:120957, 2024.

[28] Guillaume Tarel, Magnus Korpås, and Audun Botterud. Long-term equilibrium in electricity markets with renewables and energy storage only. *Energy Systems*, pages 1–23, 2024.

[29] Ying Yang, Yuting Mou, Jun Li, Beibei Wang, Changling Li, and Xiaolei Yang. Impact of capacity market mechanism on high renewable penetration systems with long-term energy storage. *Energy Conversion and Economics*, 6(5):295–307, 2025.

[30] Saman Korjani, Fabio Casu, Alfonso Damiano, Virginia Pilloni, and Alessandro Serpi. An online energy management tool for sizing integrated PV-BESS systems for residential prosumers. *Applied Energy*, 313:118765, 2022.

[31] G.X.A. Pinto, H.F. Naspolini, and R. Rüther. Assessing the economic viability of BESS in distributed PV generation on public buildings in Brazil: A 2030 outlook. *Renewable Energy*, 225:120252, 2024.

[32] Amanda Mendes Ferreira Gomes, Gustavo Xavier de Andrade Pinto, and Ricardo Rüther. Techno-economic assessment of small-size residential solar PV + battery systems under different tariff structures in Brazil. *Solar Energy*, 267:112238, 2024.

[33] Jamal Faraji, Abbas Ketabi, and Hamed Hashemi-Dezaki. Optimization of the scheduling and operation of prosumers considering the loss of life costs of battery storage systems. *Journal of Energy Storage*, 31:101655, 2020.

[34] Hedayat Saboori, Reza Hemmati, Seyyed Mohammad Sadegh Ghiasi, and Shahab Dehghan. Energy storage planning in electric power distribution networks – a state-of-the-art review. *Renewable and Sustainable Energy Reviews*, 79:1108–1121, 2017.

[35] Donal Brown, Stephen Hall, and Mark E. Davis. Prosumers in the post subsidy era: an exploration of new prosumer business models in the UK. *Energy Policy*, 135:110984, 2019.

[36] John R. Birge and François Louveaux. *Introduction to stochastic programming*. Springer, 2011.

[37] Octopus Energy. Outgoing Octopus: perfect for homes with solar panels, battery storage and other types of renewable generation., 2025.

[38] Ahmad Faruqui and Cecile Bourbonnais. The tariffs of tomorrow: Innovations in rate designs. *IEEE Power and Energy Magazine*, 18(3):18–25, 2020.

[39] Daniel Ávila, Anthony Papavasiliou, Mauricio Junca, and Lazaros Exizidis. Applying high-performance computing to the European resource adequacy assessment. *IEEE Transactions on Power Systems*, 39(2):3785–3797, 2024.

[40] Jan Figgener, Jonas Van Ouwerkerk, David Haberschusz, Jakob Bors, Philipp Woerner, Marc Mennekes, Felix Hildenbrand, Christopher Hecht, Kai-Philipp Kairies, Oliver Wessels, et al. Multi-year field measurements of home storage systems and their use in capacity estimation. *Nature Energy*, 9(11):1438–1447, 2024.

[41] Menal Guzelsoy and Theodore K Ralphs. Duality for mixed-integer linear programs. *International Journal of Operations Research*, 4(3):118–137, 2007.

[42] Yuting Mou. EV charging station data. `https://zenodo.org/records/20034739`, 2026.

[43] Nicolás Morell Dameto, José Pablo Chaves-Ávila, and Tomás Gómez San Román. Revisiting electricity network tariffs in a context of decarbonization, digitalization, and decentralization. *Energies*, 13(12), 2020.

[44] Dimitri P. Bertsekas, Gregory S. Lauer, Nils R. Sandell, and Thomas A. Posbergh. Optimal short-term scheduling of large-scale power systems. *IEEE Transactions on Automatic Control*, AC-28(1):1–11, January 1983.

[45] Nicolas Stevens, Yves Smeers, and Anthony Papavasiliou. Indivisibilities in investment and the role of a capacity market. *Journal of Regulatory Economics*, 66(2):238–272, 2024.

[46] A. Papavasiliou, Y. Mou, L. Cambier, and D. Scieur. Application of stochastic dual dynamic programming to the real-time dispatch of storage under renewable supply uncertainty. *IEEE Transactions on Sustainable Energy*, 2017.

[47] Kun Wang, Xinyi Lai, Fushuan Wen, Praveen Prakash Singh, Sambeet Mishra, and Ivo Palu. Dynamic network tariffs: Current practices, key issues and challenges. *Energy Conversion and Economics*, 4(1):23–35, 2023.

[48] Jean-Pierre Aubin and Ivar Ekeland. Estimates of the duality gap in nonconvex optimization. *Mathematics of Operations Research*, 1(3):225–245, 1976.

[49] Dimitri P Bertsekas and Nils R Sandell. Estimates of the duality gap for large-scale separable nonconvex optimization problems. In *1982 21st IEEE conference on decision and control*, pages 782–785. IEEE, 1982.

[50] Dimitri Bertsekas, G Lauer, N Sandell, and T Posbergh. Optimal short-term scheduling of large-scale power systems. *IEEE Transactions on Automatic Control*, 28(1):1–11, 1983.

[51] Steven Stoft. *Power System Economics*. IEEE Press and Wiley Interscience, 2002.